Bioorganic Chemistry 92 (2019) 103203

Contents lists available at ScienceDirect

Bioorganic Chemistry

journal homepage: www.elsevier.com/locate/bioorg

Nusbiarylins, a new class of antimicrobial agents: Rational design of bacterial transcription inhibitors targeting the interaction between the NusB and NusE proteins

Yangyi Qiu[a,b], Shu Ting Chan[a,b], Lin Lin[c], Tsun Lam Shek[d], Tsz Fung Tsang[c], Yufeng Zhang[d], Margaret Ip[c], Paul Kay-sheung Chan[c,e], Nicolas Blanchard[f], Gilles Hanquet[g], Zhong Zuo[d,*], Xiao Yang[c,*], Cong Ma[a,b,*]

[a] The Hong Kong Polytechnic University Shenzhen Research Institute, Shenzhen, China
[b] State Key Laboratory of Chemical Biology and Drug Discovery, Department of Applied Biology and Chemical Technology, The Hong Kong Polytechnic University, Kowloon, Hong Kong Special Administrative Region
[c] Department of Microbiology, The Chinese University of Hong Kong, Prince of Wales Hospital, Shatin, Hong Kong Special Administrative Region
[d] School of Pharmacy, Faculty of Medicine, The Chinese University of Hong Kong, Shatin, New Territories, Hong Kong Special Administrative Region
[e] Stanley Ho Centre for Emerging Infectious Diseases, The Chinese University of Hong Kong, Shatin, Hong Kong Special Administrative Region
[f] Université de Haute-Alsace, Université de Strasbourg, CNRS, LIMA, UMR 7042, Mulhouse 68000, France
[g] Laboratoire d'Innovation Moléculaire et Applications, ECPM, UMR 7042, Université de Strasbourg/Université de Haute-Alsace, CNRS, 67000 Strasbourg, France

ARTICLE INFO

Keywords:
Bacterial transcription
Protein-protein interaction
NusB
Inhibitor
Antimicrobial activity

ABSTRACT

Discovery of antibiotics of a novel mode of action is highly required in the fierce battlefield with multi-drug resistant bacterial infections. Previously we have validated the protein-protein interaction between bacterial NusB and NusE proteins as an unprecedented antimicrobial target and reported the identification of a first-in-class inhibitor of bacterial ribosomal RNA synthesis with antimicrobial activities. In this paper, derivatives of the hit compound were rationally designed based on the pharmacophore model for chemical synthesis, followed by biological evaluations. Some of the derivatives demonstrated the improved antimicrobial activity with the minimum inhibitory concentration (MIC) at 1–2 μg/mL against clinically significant bacterial pathogens. Time-kill kinetics, confocal microscope, ATP production, cytotoxicity, hemolytic property and cell permeability using Caco-2 cells of a representative compound were also measured. This series of compounds were named "nusbiarylins" based on their target protein NusB and the biaryl structure and were expected to be further developed towards novel antimicrobial drug candidates in the near future.

1. Introduction

Staphylococcus aureus is one of the most important Gram-positive pathogens leading to a series of conditions ranging from mild skin and soft tissue infections, respiratory infections, to fatal sepsis [1]. The re-emergence of methicillin-resistant *S. aureus* (MRSA) infections which render commonly used antibiotic treatment less effective has become a threat to public health [2]. MRSA infections could occur in hospitals or other health care settings, known as healthcare-associated (HA) MRSA or community-associated among healthy populations (CA-MRSA) [2]. Discovery of structurally novel antimicrobial agents with distinct target and mechanisms capable of eliminating MRSA is urgently required, as they will provide alternative therapeutic choices for clinical management of infections caused by the resistant pathogens.

Bacterial transcription has been a proven target for antibiotics with two drugs rifamycin and fidaxomicin in current clinical use [3]. Transcription is carried out by a multi-subunit RNA polymerase (RNAP), composed by two α subunits holding β and β' subunits to form the catalytic center and small subunits ω and/or ε [4,5] There are a number of transcription factors involved in the transcription regulation, among which is the *N*-utilization substances (Nus) factor family consisting of NusA, NusB, NusE (ribosomal protein S10) and NusG [6,7]. The Nus

* Corresponding authors at: The Hong Kong Polytechnic University Shenzhen Research Institute, Shenzhen, China, and State Key Laboratory of Chemical Biology and Drug Discovery, Department of Applied Biology and Chemical Technology, The Hong Kong Polytechnic University, Kowloon, Hong Kong Special Administrative Region (C. Ma); Department of Microbiology, The Chinese University of Hong Kong, Prince of Wales Hospital, Shatin, Hong Kong Special Administrative Region (X. Yang); School of Pharmacy, Faculty of Medicine, The Chinese University of Hong Kong, Shatin, New Territories, Hong Kong Special Administrative Region (Z. Zuo).
E-mail addresses: joanzuo@cuhk.edu.hk (Z. Zuo), xiaoyang@cuhk.edu.hk (X. Yang), cong.ma@polyu.edu.hk (C. Ma).

https://doi.org/10.1016/j.bioorg.2019.103203
Received 20 May 2019; Received in revised form 15 July 2019; Accepted 14 August 2019
Available online 16 August 2019

factors were first described as part of the antitermination complex for λ bacteriophage RNA synthesis [8–11], and they were also responsible for the efficient transcription of bacterial ribosomal RNA (rRNA) operons [12–14]. Other than transcription regulation, the Nus factors are responsible for the coupling of transcription and translation in bacterial cells [15]. Recently, the Nus factors have also been shown to be involved in rRNA folding and ribosome biogenesis [16].

The NusB and NusE proteins are relatively small in size (< 15 kDa) and the formation of NusB-NusE heterodimer is the first step in the formation of the bacterial rRNA operon transcription complex [17]. Since NusB and NusE are highly conserved and essential for bacterial cell viability, we hypothesize that small molecules disrupting NusB–-NusE heterodimer formation will result in antimicrobial activities. Recently, we reported the discovery of a first-in-class inhibitor against bacterial ribosomal RNA synthesis, targeting the NusB and NusE protein-protein interaction (PPI) [18]. The hit compound **14** was identified by an *in silico* screening of a pharmacophore model designed based on the crystal structures of NusB and NusE heterodimer [19]. **14** has been shown to have antimicrobial activity against *S. aureus* strains including MRSA [18]. In this paper, chemical derivatives of **14** were rationally designed and synthesized and followed by the assessment of their antimicrobial activities.

2. Results and discussion

2.1. Design and synthesis

The chemical modifications have been designed to examine the interaction of the left and right benzene ring of analogs of the hit compound **14** with NusB [20], but the effect of more diverse substitution on the left benzene ring and the linker to the inhibitory and antimicrobial activities needs to be investigated (Fig. 1A). We considered the substitution on the left benzene ring of **14** could be altered to achieve the improved binding with NusB, for which the linker between the two benzene rings of **14** may also play an important role to position the left benzene ring when the right benzene ring was anchored by two hydrogen bonds (Fig. 1B). The nitro group and hydroxyl of phenolic alcohol on the right benzene ring were designed to be kept intact to maintain the important hydrogen bonds between the right benzene ring of hit compound with Tyr16 and Glu81 of NusB, respectively (Fig. 1B).

2-hydroxy-5-nitrobenzaldehyde was subjected to condensation with various primary amine compounds **1a-16a** to provide the desired imines **1–16** in 60–93% yields (Scheme 1). Reduction of imines furnished amine analogs **17–31** in 84–94% yields.

To synthesize the analogs with a C=C double bond linker, the hydroxyl of the same starting material above was first protected as ether **32a** to undergo a Horner–Wadsworth–Emmons reaction, followed by the deprotection of **32b** to give olefin **32** (Scheme 2). Ether **32a** was converted to olefin **33a** by a Wittig reaction, which was subjected to Heck reaction with substituted iodobenzenes **33b-37b** to give **33c-37c** (Scheme 2). The deprotection of ether provided olefins **33–37** in 58–67% yields. Amide **38** was also synthesized in 74% yield by a simple amidation of amine **14a**, and ketone **39** was obtained in 74% yield by a palladium-catalyzed coupling reaction between iodobenzene and aldehyde (Scheme 2).

2.2. Antimicrobial activity and target PPI inhibition

The antimicrobial activity of the compounds was firstly tested following the Clinical & Laboratory Standards Institute CLSI procedures using *S. aureus* ATCC 25923, which is a type strain for antimicrobial susceptibility test [21]. Inhibition of the compounds on the *in vitro* NusB-NusE interaction was assessed by an in-house designed split-luciferase assay [22]. NusB and NusE were each tagged with one of the luciferase complementation fragments and formation of the heterodimer in the presence of the inhibitors will be measured by luminescence released from the reformation of native luciferase [22]. The result was expressed as % inhibition normalized to the control groups without compound treatment. The results of compounds **1–31** with the imine and amine linkers are shown in Table 1. When the substituents on the left benzene ring of compounds are an atom such as fluoride in compounds **1–3** and a simple methyl group in **4–6**, the MIC values ranged 4–8 μg/mL close to the hit compound **14**, and the inhibition of compounds on the NusB-NusE interaction was slightly inferior to **14** (Table 1). When the imine linker was reduced to amine, the resulting compounds **17–22** demonstrated equal or decreased inhibitory and antimicrobial activities (MICs 8–32 μg/mL; Table 1). On the contrast, imine compounds **7–16** with bulkier substituents such as methoxy, carboxylate, and hydroxymethyl displayed equal (Compound **8**) or inferior inhibitory activity and increased antimicrobial activity (MICs 2–4 μg/mL), while amine homologs always had reduced antimicrobial activity (MICs 32–256 μg/mL; Table 1). The results suggested that the bulky substituents were preferred for improved activity, and the flexible conformation may generate the entropy penalty to affect the activity of compounds. The only exception is compound **7** with a very bulky *t*-butyl group, the reduction of imine linker to amine gave **23** which demonstrated an improved MIC of 2 μg/mL (Table 1).

Compounds **32–39** with various linkers have also been examined to display diverse inhibitory and antimicrobial activities (Table 2). Compared to compounds **8** and **9** with the imine linker, olefin compounds **33** and **34** expressed similar antimicrobial activity (Table 2). On the contrast, olefins **36** and **37** exhibited lower activity than imine homologs **12** and **13**. The best inhibitory activity was obtained with compound **38** with a 3-ethynyl group on the left benzene ring same to the hit compound **14** (Table 2). This compound contains an amide linker to provide an equal antimicrobial activity to **14**. Finally, **39** with a carbonyl linker displayed a reduced inhibitory and antimicrobial activity (Table 2). In summary, the imine linker of this class of diaryl compounds can be changed to other chemical groups to increase the chemical diversity, but the distance of linker needs to be maintained with at least two atoms.

Based on the structural feature of diaryl group and the universal antimicrobial activity associated to this structure, as well as the target specificity on the surface of the NusB protein, we intended to name this

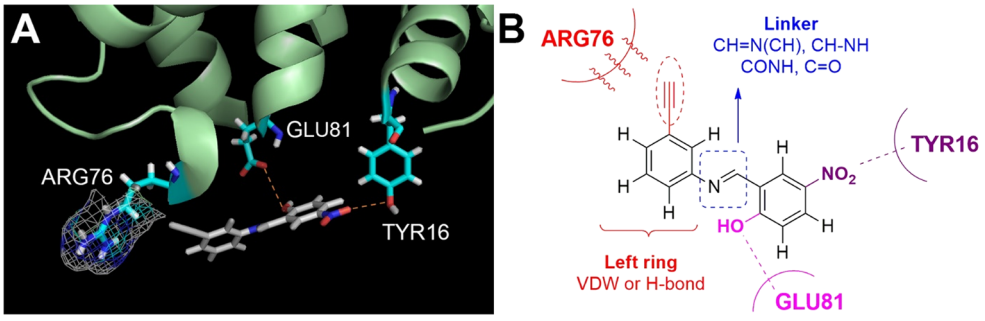

Fig. 1. (A) Binding model of **14** with its target protein NusB. (B) Design of derivatives of **14**.

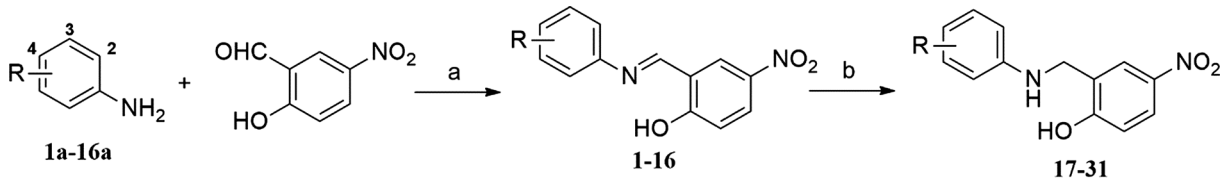

	R		R
1a, 1, 17	2-F	**9a, 9, 25**	3-OCH_3
2a, 2, 18	3-F	**10a, 10, 26**	4-OCH_3
3a, 3, 19	4-F	**11a, 11, 27**	2-$COOCH_3$
4a, 4, 20	2-CH_3	**12a, 12, 28**	3-$COOCH_3$
5a, 5, 21	3-CH_3	**13a, 13, 29**	4-$COOCH_3$
6a, 6, 22	4-CH_3	**14a, 14, 30**	3-ethynyl
7a, 7, 23	3-$C(CH_3)_3$	**15a, 15, 31**	3-CH_2OH
8a, 8, 24	2-OCH_3	**16a, 16**	4-CH_2OH

Reagents and conditions: (a) EtOH, rt, overnight, 60-93%; (b) $NaBH(OAc)_3$, DCM, rt, overnight, 84-94%

Scheme 1. Synthesis of imines **1–16** and amines **17–31.**

class of compounds as "nusbiarylins". To better explore the potential of nusbiarylins, we examined the antibacterial spectrum of these compounds. The first bacteria set used is the top six pathogens amongst the most recent "WHO priority pathogens list for guiding R&D of new antibiotics" containing three Gram-positive and three Gram-negative bacteria: *Enterococcus faecium*, *S. aureus*, *Streptococcus pneumonia*, *Acinetobacter baumannii*, *Pseudomonas aeruginosa*, and *Enterobacter* spp. We used the standard strains for antibiotic susceptibility testing and the CLSI recommended conditions to perform the experiment [20]. The compounds demonstrated the preferred antimicrobial activity against the Gram-positive than Gram-negative pathogens with specific activities against *S. aureus*, *S. pneumonia* and *E. faecium* (Table S1). Gram-negative bacteria were less responsive to the nusbiarylin compound treatment, which may due to reduced permeability and vigorous efflux system. Further synthesis and biological investigation will be carried out in the near future. Encouragingly, modest antimicrobial activity was observed against the *A. baumannii* strain (MIC 32 μg/mL; Table S1). As *A. baumannii* is top one bacterium of the WHO pathogen list that requires new antibiotic development, our compounds may be developed as a specific antimicrobial agent to address this urgent need.

A series of compounds were then chosen to test against representative clinically significant Gram-positive pathogens such as *Enterococcus casseliflavus* causing bacteremia [23], *Staphylococcus epidermidis* able of growing biofilms on plastic devices, most commonly on intravenous catheters [24], *Staphylococcus saprophyticus* causing urinary tract infections [25], *S. pneumoniae* as the major cause of community acquired pneumonia and meningitis [26], *Streptococcus pyogenes* (Group A *Streptococcus*, GAS) causing pharyngitis (strep throat), localized skin infection (impetigo), necrotizing fasciitis, and neonatal infections [27], *Streptococcus agalactiae* (Group B *Streptococcus*, GBS) causing neonatal infections [28]. As shown in Fig. 2A, some of the compounds displayed antibacterial activity against all of these Gram-positive pathogens with clinical complexity for treatment, especially compound **23** displayed a significant antimicrobial activity against *Staphylococcus saprophyticus* ATCC 15305 with an MIC of 1 μg/mL, which demonstrated the potentials of our compounds.

MRSA represents one of the most difficult bacterial strains for treatment due to antibiotic resistance [2]. We also tested the above compounds against a series of globally spread HA- and CA-MRSA strains. All of the compounds displayed consistent antibacterial activity against the *S. aureus* strains with the best MIC as low as 2 μg/mL (Fig. 2B), in which most of them developed resistance to oxacillin, the first-line antibiotic drug used in the USA for MRSA. Our compounds were able to maintain stable MIC values against diverse MRSA strains, suggesting the compounds may be developed further with improved antimicrobial activity to treat MRSA infections.

2.3. Time-kill kinetic

The time-kill kinetic assay assesses the *in vitro* activity of an antimicrobial agent against a bacterial strain over time and was performed according to the CLSI guidelines [20]. The time kill kinetics of compound **23** was measured against *S. aureus* ATCC 25923 in liquid culture. **23** demonstrated growth inhibition at the ¼ and 1 × MIC and started to reduce the CFU (colony forming unit) counts at 4 × MIC (Fig. 3A). When higher concentrations of **23** were used in this experiment, *S. aureus* could be totally and efficiently eradicated below the theoretical level of detection (200 CFU/mL) in 2 h, 16 h, and 20 h using 32, 16 and 8 × MIC, respectively (Fig. 3A). The result suggested that the compounds were bacteriostatic at lower concentrations and became bactericidal at higher concentration in a very short time.

2.4. ATP production

It was reported that inhibition of bacterial central metabolism is related to antimicrobial efficacy [29]. Therefore, we have examined compound **23** on its function to interfere with bacterial metabolism by measuring the level of ATP in *S. aureus* ATCC 29523 cells over time in the presence of **23** at various concentrations. When **23** was used at ¼ or 1 × MIC, impaired ATP production could be observed as compared to untreated cells. As proteins already existing in cells were still capable of functioning as normal cells even transcription is inhibited, treatment of **23** at 4 × MIC obstructed cell respiration within 2 h. Another transcription-targeting antimicrobial agent, rifampicin has been shown to suppress the oxygen consumption rate in *S. aureus* cells, which is consistent with our observation with nusbiarylins [29].

2.5. Cellular effect of nusbiarylin compounds

To study the mechanism of the nusbiarylin compounds at the cellular level, a *Bacillus subtilis* strain named BS61 was employed, which contains a green fluorescent protein (*gfp*) fusion to the *nusB* gene on the chromosomal copy [30]. The subcellular localization of NusB fluorescence in the control group could be clearly identified under the confocal microscope at the sub-nucleoid regions called transcription foci (Fig. 4A Ctrl) [30]. When the cells were treated with compound **23** at 1/

Preparation of **32**

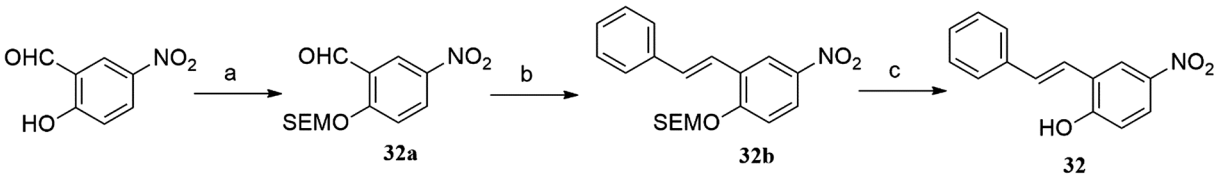

Preparation of **33-37**

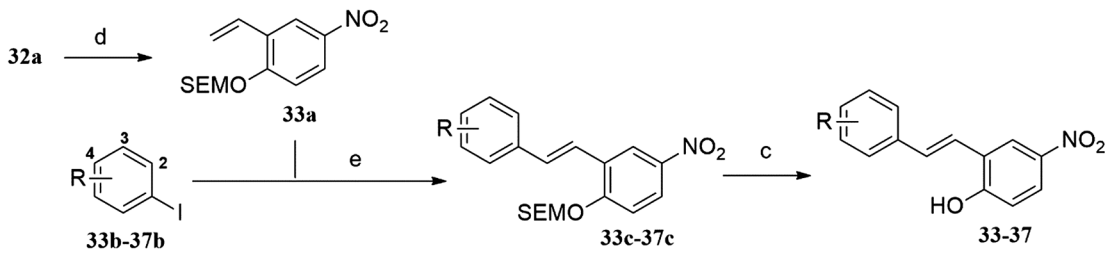

	R
33b, 33c, 33	2-OCH_3
34b, 34c, 34	3-OCH_3
35b, 35c, 35	2-CN
36b, 36c, 36	3-$COOCH_3$
37b, 37c, 37	4-$COOCH_3$

Preparation of **38**

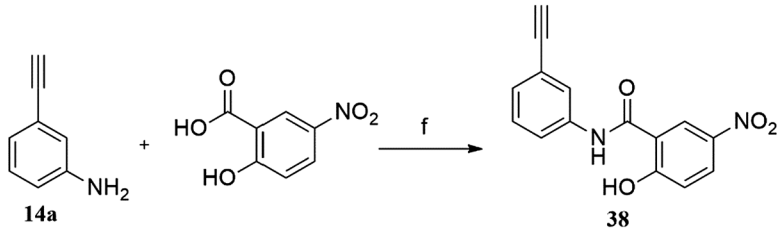

Preparation of **39**

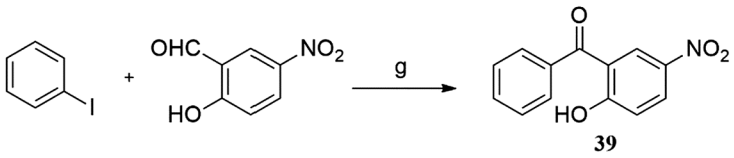

Reagents and conditions: (a) SEMCl, DIPEA, DCM, rt, 3h, 80%; (b) diethyl benzylphosphonate, NaH, THF, rt, overnight; (c) 2% H_2SO_4-MeOH, rt, overnight, 58-67%; (d) methyltriphenylphosphonium bromide, NaH, THF, overnight, 62%; (e) K_3PO_4, $Pd(OAc)_2$, DMF, 100°C, overnight; (f) triphenyl phosphite, toluene, reflux, 6h, 74%; (g) $PdCl_2$, LiCl, Na_2CO_3, DMF, 120°C, 6h, 74%

Scheme 2. Synthesis of olefins **32–37**, amide **38** and ketone **39**.

8 × MIC for 15 min, diffusion of the fluorescent signal into the cytosol could already be observed although there were still localizations at the nucleoids (Fig. 4A). When **23** was used at ¼ × MIC, the nucleoid could barely be seen, and the cytosolic regions were filled with fluorescence (Fig. 4A). When **23** was used at ½ or 1 × MIC, no nucleoid could be observed, suggesting disruption of NusB localization by the nusbiarylin compound treatment (Fig. 4A). The level of macromolecules in *B subtilis* cells due to **23** treatment at a sub- MIC level (1/8 MIC and 1/4 MIC) unaffecting cell growth was also measured (Fig. 4B). *B. subtilis* cells were subject to **23** treatment at early log-phase (OD 0.2), and harvested and lysed at mid-log phase (OD 0.5) for macromolecular quantitation. While the DNA levels were not affected as predicted by the mode of action, **23** showed a significant reduction in the RNA and rRNA level compared with the untreated control cells (Fig. 4B).

2.6. In vitro cytotoxicity

Some compounds with the MIC values of 2 μg/mL against *S. aureus* ATCC 25923 were chosen for *in vitro* cytotoxicity testing as described previously [18]. Cell lines A549 human lung carcinoma and HaCaT

Table 1
Inhibitory and antimicrobial activities of compounds **1–31**

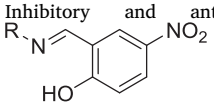

1-16

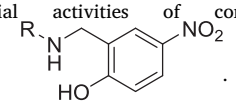

17-31

Compound	R	MIC (μg/mL)	NusB/E PPI % Inhibition	ClogP
1		8	73.4 ± 2.0	3.36
17		8	64.0 ± 5.2	3.20
2		4	65.4 ± 3.2	3.36
18		16	37.5 ± 7.1	3.20
3		8	59.2 ± 2.0	3.36
19		32	66.0 ± 2.2	3.20
4		4	53.1 ± 1.3	3.55
20		8	46.1 ± 6.7	3.25
5		4	54.9 ± 2.8	3.55
21		16	44.4 ± 6.2	3.25
6		4	49.2 ± 0.9	3.55
22		16	36.1 ± 6.4	3.25
7	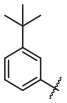	4	51.3 ± 1.5	4.88
23		2	39.5 ± 2.7	4.58
8		2	82.6 ± 0.8	3.07
24		32	45.2 ± 7.9	2.85
9		2	68.0 ± 0.8	3.07
25		64	34.9 ± 10.3	2.85
10	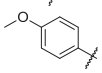	4	61.8 ± 2.8	3.07
26		128	48.2 ± 7.8	2.85
11	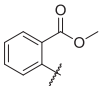	4	72.5 ± 3.3	3.33
27		128	13.0 ± 5.7	3.77
12	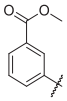	2	48.1 ± 3.1	3.33
28		32	14.6 ± 10.7	3.27
13	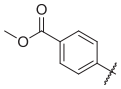	2	61.8 ± 3.3	3.33
29		> 256	16.8 ± 2.6	3.27
14	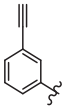	8	85.3 ± 1.5	3.32
30		16	47.7 ± 7.9	3.02
15	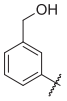	4	70.6 ± 1.8	2.01
31		256	61.4 ± 4.3	1.73
16		4	72.6 ± 2.6	2.01

human keratinocytes were used as the infections caused by *S. aureus* often occur in lung and skin tissues. The 50% cytotoxic concentration (CC_{50}) was defined as a compound's concentration required for the reduction of cell viability by 50%. Compounds **8, 9, 12, 13** with the imine linker did not show any cytotoxicity (CC_{50} > 200 μM, table 3), whereas compounds **23** and **34** with an amine and olefin linkers respectively demonstrated very mild cytotoxicity (CC_{50} 18–34 μM). The therapeutic index (TI) is a quantitative measurement of the relative

Table 2
Inhibitory and antimicrobial activities of compounds **32–39**

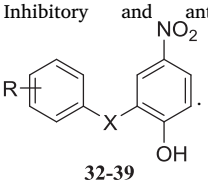

32-39

Compound	R	X	MIC (μg/mL)	NusB/E PPI % Inhibition	ClogP
32	H	(*E*)-CH=CH-	2	56.6 ± 6.4	4.54
33	2-OCH_3	(*E*)-CH=CH-	4	41.6 ± 4.8	4.47
34	3-OCH_3	(*E*)-CH=CH-	2	70.3 ± 4.4	4.47
35	2-CN	(E)-CH=CH-	8	44.9 ± 3.5	3.98
36	3-$COOCH_3$	(*E*)-CH=CH-	64	24.6 ± 6.7	4.52
37	4-$COOCH_3$	(*E*)-CH=CH-	128	41.7 ± 3.7	4.52
38	3-C≡CH	-NHCO-	8	99.2 ± 0.2	3.83
39	H	-CO-	64	41.3 ± 5.3	3.59

safety of a drug. TI was defined as the ratio that compares the effective concentration and the concentration at which the drug became toxic and the TI was promising with 53–153 for imines, 6–9 for amine **23** and olefin **34**. Note that the TI was very preliminary by comparing the cell-based cytotoxicity of compounds to antimicrobial activity, which needs more validation using the *in vivo* animal models in further research. Nevertheless, this class of compounds is potential for further studies.

2.7. In vitro pharmacology

With the antibacterial activity in hand, we intended to explore the *in vitro* pharmacological properties of these compounds. We first investigated whether the compounds would cause hemolysis when injected into the blood veins [31]. The hemolytic activities against human blood cells of compound **23** were tested. As shown in Fig. 5, compound **23** demonstrated almost no hemolytic potential compared to the suggested nonhemolytic cut-off value (< 10%) at all tested concentrations (0.1, 1 and 10 μg/mL).

For drugs that are orally available, the intestinal absorption is critical. The human intestinal epithelial cancer cell line Caco-2 was used to determine the permeability of compound **23** [31]. As shown in Table 4, compound **23** possessed an excellent cell permeability, which is superior to 1×10^{-5} cm/s as the standard of great intestinal epithelial cell permeability. Furthermore, the deduced apparent permeability of compounds had a similar magnitude to that of the predicted value by pkCSM [32].

3. Conclusions

In this paper, we described the rational design and chemical synthesis of a new class of diaryl compounds based on the previously established hit compound and the pharmacophore model. The inhibitory activity at the molecular level against the *in vitro* NusB-NusE heterodimer formation together with the antimicrobial activity confirmed the rationales of the compound design. Further characterizations by time-kill kinetics, ATP production, and confocal microscopy provided more information on the antimicrobial activity and the mechanism at the cellular level. The cytotoxicity and *in vitro* pharmacology study demonstrated that these compounds are suitable for further drug development. The new series of compounds named nusbiarylin is a new class of antimicrobial agent targeting a new PPI in bacteria, with a distinct mechanism of action as compared with the current antibiotics on the market. We believe further studies on these compounds will contribute to a new era of antibiotic discovery.

A

	ECAS	SEPI	SSAP	SPNE	SPYO	SAGA
6	>256	32	>256	128	>256	>256
8	>256	16	256	32	256	>256
9	>256	16	256	64	>256	>256
13	128	4	128	16	128	128
14	>256	16	256	32	256	256
16	>256	16	256	64	256	>256
23	32	16	1	8	16	16
34	32	4	8	8	16	16
CIP	4	0.0625	0.5	0.5	0.5	4
GEN	4	0.125	0.0625	32	8	32
OXA	32	0.25	1	2	0.0625	0.5
VAN	4	1	1	0.5	0.5	0.5

μg/ml ≤1 2 4 8 16 32-64 >256

B

	25923	29213	ST 239	BAA -43	BAA -44	ST 45	ST 30	45 ST59	46 ST59	USA 300	ST 22	ST 338	ST 217	ST 5
6	4	16	16	16	16	16	32	16	16	8	8	8	8	8
8	2	8	16	16	16	16	8	8	16	8	8	8	8	8
9	2	8	8	8	32	16	16	16	16	8	8	8	8	8
14	8	16	16	8	32	32	16	16	16	16	16	16	8	8
16	4	8	8	8	16	16	16	16	16	8	8	8	8	8
23	2	4	8	2	8	8	4	8	8	8	8	4	4	4
34	2	2	4	4	4	4	4	4	4	4	4	4	4	4
CIP	1	1	4	2	4	2	0.5	0.25	0.25	4	4	0.5	4	4
GEN	1	1	>256	>256	>256	16	0.25	0.5	0.5	0.5	0.25	0.25	0.5	>256
OXA	1	0.25	>256	>256	>256	4	4	8	8	32	64	0.5	64	>256
VAN	2	1	1	1	1	0.5	0.5	0.5	1	1	0.5	0.5	0.5	0.5

Fig. 2. Antimicrobial activity evaluation of the nusbiarylin compounds with the MICs (μg/mL) shown against (A) Representative Gram-positive pathogens and (B) *S. aureus* including representative globally spread HA- and CA-MRSA strains. ECAS, *Enterococcus casseliflavus* ATCC 25788, SEPI, *Staphylococcus epidermidis* ATCC 12228, SSAP, *Staphylococcus saprophyticus* ATCC 15305, SPNE, *S. pneumoniae* ATCC 49619, SPYO, *Streptococcus pyogenes* ATCC 19615, SAGA, *Streptococcus agalactiae* ATCC 12386, CIP, ciprofloxacin, GEN, gentamicin, OXA, oxacillin, VAN, vancomycin.

4. Experimental section

4.1. Materials and chemicals

Sodium Chloride and Phosphate Buffered Saline (tablets) were purchased from Sigma-Aldrich (Saint Louis, Missouri). GR Grade Dimethyl Sulfoxide (DMSO) was purchased from Duksan Pure Chemicals (Ansan City, South Korea) and HPLC Grade Acetonitrile was purchased from Merck KGaA (Darmstadt, Germany). For 150 mM NaCl buffer, 4.383 g of NaCl crystals were dissolved in 500 mL of Milli-Q water. 1x PBS was prepared by dissolving 1 PBS tablet into 200 mL of Milli-Q water. Antibiotics were purchased from Sigma-Aldrich (Saint Louis, Missouri).

4.2. Chemistry

4.2.1. General procedure (A) for the synthesis of Schiff base type derivatives

To a solution of benzaldehydes (1 equiv) in ethanol (10 mL) was added anilines (1 equiv), and the reaction mixture was stirred at room temperature overnight. The solid was collected by filtration and washed with cold ethanol and hexane.

4.2.2. General procedure (B) for the synthesis of aniline type derivatives

To a solution of Schiff base type derivatives (1 equiv) obtained according to general procedure (A) in DCM (10 mL) was added sodium triacetoxyborohydride (3 equiv), and the reaction mixture was stirred at room temperature overnight. The crude reaction mixture was

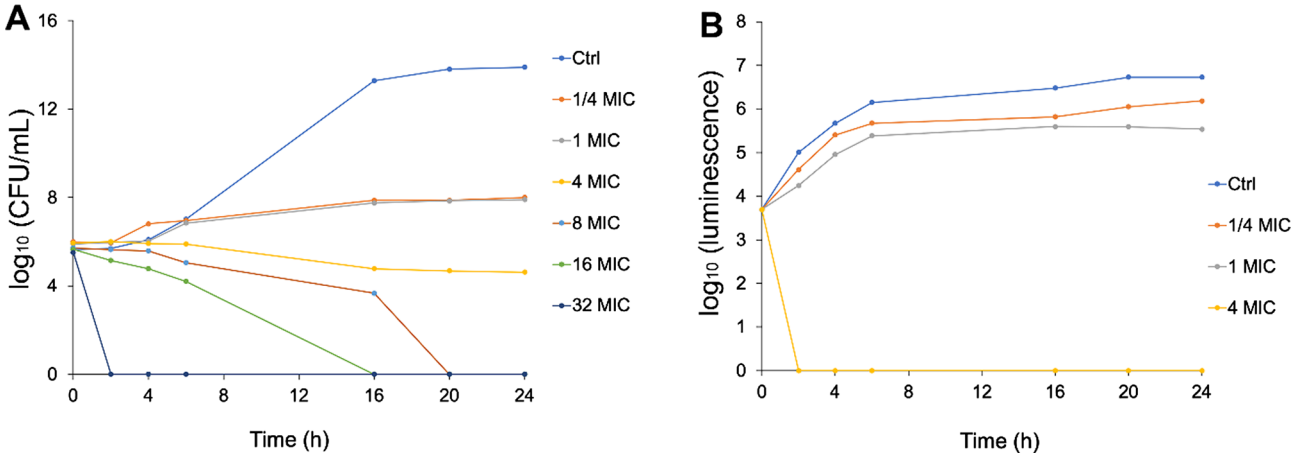

Fig. 3. The effect of nusbiarylin compounds on *S. aureus* growth and metabolism. (A) Time kill kinetics of *S. aureus* treated with **23** at different concentrations. (B) The ATP production of *S. aureus* treated with **23** at different concentrations.

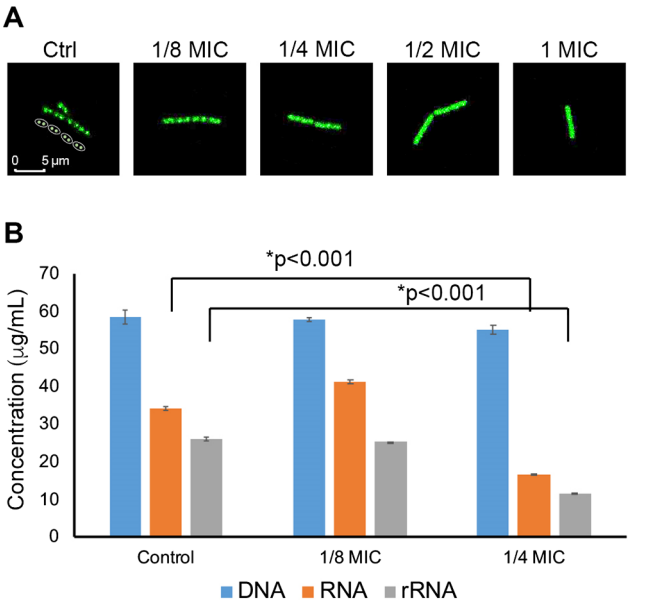

Fig. 4. (A) Confocal microscope of *B. subtilis* with NusB fluorescence and **(B)** the level of DNA, RNA and rRNA in *B. subtilis* cells treated by compound **23** at different concentrations.

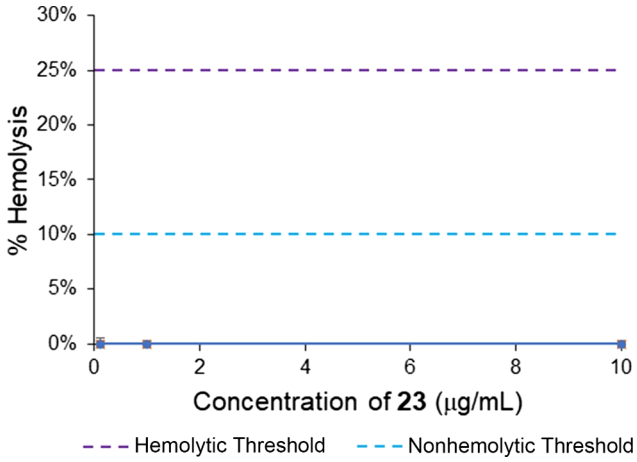

Fig. 5. *In vitro* hemolysis activity of compound **23** (blue line on the bottom).

Table 3
Cytotoxicity of selective compounds against human A549 and HaCaT cell lines.

Cpd.	MIC[a] (μg/mL)	CC_{50} (μM)		Therapeutic Index[b]	
		A549	HaCaT	A549	HaCaT
8	2	454.40 ± 27.45	438.94 ± 24.81	124	120
9	2	232.10 ± 9.46	195.82 ± 23.08	63	53
12	2	446.51 ± 28.56	391.59 ± 25.80	134	118
13	2	510.42 ± 29.40	381.19 ± 24.41	153	114
23	2	18.32 ± 1.75	20.24 ± 2.42	6	6
34	2	34.58 ± 4.06	30.51 ± 3.43	9	8
DDP[c]	–	7.70 ± 0.58	7.83 ± 0.66	–	–

[a] *S. aureus* ATCC 25923.
[b] Calculated by CC_{50} (μg/mL)/½ MIC (μg/mL).
[c] DDP: cisplatin.

Table 4
The deduced and predicted apparent permeability of compound **23.**

Compound	P_{app} Average (n = 4) (cm/s)	P_{app} Predicted (cm/s)
23	$1.87 \pm 0.47 \times 10^{-5}$	8.09×10^{-6}

evaporated *in vacuo* and the pure product was obtained after flash chromatography.

4.2.3. General procedure (C) for synthesis of (E)-stilbenes

Step 1: Hydroxyl group-protected (E)-stilbenes. To a mixture of trimethyl(2-((4-nitro-2-vinylphenoxy)methoxy)ethyl)silane (**33a**) (1.2 equiv), K_3PO_4 (1.4 equiv) and $Pd(OAc)_2$ (0.03 equiv) in a sealed tube was added iodobenzenes (1.0 equiv) and anhydrous DMF (3 mL) in glovebox. The resulting mixture was stirred at 100 °C overnight. After the reaction mixture was cooled to room temperature, the product was extracted with EtOAc (30 mL × 3). The organic layers were combined, washed with saturated brine, dried over Na_2SO_4 and filtered. All volatiles were removed under reduced pressure and the crude product containing 2–5% isomer was isolated by flash chromatography (EtOAc/Hex) on silica gel.
Step 2: To a solution of crude product obtained above in MeOH (10 mL) was added H2SO4 (100 μL). The mixture was stirred at rt overnight. After the reaction was completed, the product was extracted with EtOAc (30 mL × 3). The organic layers were combined, washed with saturated brine, dried over Na2SO4 and filtered. All volatiles were removed under reduced pressure and the title product was isolated by flash chromatography (EtOAc/Hex) on silica gel.

4.2.4. (E)-2-(((2-fluorophenyl)imino)methyl)-4-nitrophenol (1)

The title compound was prepared according to general procedure (**A**) using 5-nitrosalicylaldehyde (200 mg, 1.20 mmol) and 2-fluoroaniline **1a** (116 μL, 1.20 mmol, 1 equiv), yielding the pure product as a yellow solid (201 mg, 65%); ^{1}H NMR (400 MHz, Chloroform-*d*) δ 14.25 (s, 1H), 8.85 (s, 1H), 8.43 (d, J = 2.8 Hz, 1H), 8.31 (dd, J = 9.2, 2.8 Hz, 1H), 7.40 – 7.32 (m, 2H), 7.28 – 7.23 (m, 2H), 7.15 (d, J = 9.2 Hz, 1H); ^{13}C NMR (100 MHz, Chloroform-*d*) δ 166.7, 162.4 (d, J = 3.0 Hz), 155.9 (d, J = 253.5 Hz), 140.0, 134.6 (d, J = 9.1 Hz), 129.2 (d, J = 8.1 Hz), 128.5 (d, J = 10.1 Hz), 124.9 (d, J = 4.0 Hz), 121.3, 118.4, 118.2, 116.9 (d, J = 19.2 Hz); HRMS (ESI) calcd for $C_{13}H_8FN_2O_3$ (M - H^+) 259.0524, found 259.0523; Melting Point: 166–167 °C.

4.2.5. (E)-2-(((3-fluorophenyl)imino)methyl)-4-nitrophenol (2)

The title compound was prepared according to general procedure (**A**) using 5-nitrosalicylaldehyde (200 mg, 1.20 mmol) and 3-fluoroaniline **2a** (115 μL, 1.20 mmol, 1 equiv), yielding the pure product as a yellow solid (230 mg, 74%); ^{1}H NMR (400 MHz, Chloroform-*d*) δ 14.03 (s, 1H), 8.73 (s, 1H), 8.43 (d, J = 2.8 Hz, 1H), 8.31 (dd, J = 9.1, 2.7 Hz, 1H), 7.49 – 7.43 (m, 1H), 7.15 – 7.06 (m, 4H); ^{13}C NMR (100 MHz, Chloroform-*d*) δ 166.5, 163.4 (d, J = 249.5 Hz), 161.8, 148.7 (d, J = 8.9 Hz), 140.2, 131.0 (d, J = 9.1 Hz), 128.6 (d, J = 10.1 Hz), 118.4, 118.0, 117.1 (d, J = 3.0 Hz), 114.9 (d, J = 21.2 Hz), 108.6 (d, J = 23.2 Hz); HRMS (ESI) calcd for $C_{13}H_8FN_2O_3$ (M - H^+) 259.0524, found 259.0828; Melting Point: 172–173 °C.

4.2.6. (E)-2-((((4-fluorophenyl)imino)methyl)-4-nitrophenol (3)

The title compound was prepared according to general procedure (**A**) using 5-nitrosalicylaldehyde (200 mg, 1.20 mmol) and 4-fluoroaniline **3a** (114 μL, 1.20 mmol, 1 equiv), yielding the pure product as a yellow solid (195 mg, 63%); ^{1}H NMR (400 MHz, Chloroform-*d*) δ 14.24 (s, 1H), 8.71 (s, 1H), 8.42 (d, J = 2.8 Hz, 1H), 8.30 (dd, J = 9.2, 2.8 Hz, 1H), 7.37 – 7.34 (m, 2H), 7.22 – 7.14 (m, 2H), 7.13 (d, J = 9.2 Hz, 1H); ^{13}C NMR (100 MHz, DMSO-d_6) δ 166.7, 161.8, 161.8 (d, J = 245.4 Hz), 143.7 (d, J = 3.0 Hz), 139.7, 128.8, 128.6, 123.9 (d, J = 9.1 Hz), 119.2, 118.6, 116.8 (d, J = 23.2 Hz); HRMS (ESI) calcd for $C_{13}H_8FN_2O_3$ (M - H^+) 259.0524, found 259.0522; Melting Point: 196–197 °C.

4.2.7. (E)-4-nitro-2-((o-tolylimino)methyl)phenol (4)

The title compound was prepared according to general procedure (**A**) using 5-nitrosalicylaldehyde (200 mg, 1.20 mmol) and 2-methylaniline **4a** (128 μL, 1.20 mmol, 1 equiv), yielding the pure product as a yellow solid (215 mg, 70%); ^{1}H NMR (400 MHz, Chloroform-*d*) δ 14.74 (s, 1H), 8.70 (s, 1H), 8.44 (d, J = 2.8 Hz, 1H), 8.30 (dd, J = 9.2, 2.8 Hz, 1H), 7.36 – 7.28 (m, 3H), 7.21 – 7.18 (m, 1H), 7.13 (d, J = 9.1 Hz, 1H), 2.46 (s, 3H); ^{13}C NMR (100 MHz, Chloroform-*d*) δ 167.2, 160.2, 145.6, 139.9, 132.6, 131.1, 128.4, 128.3, 128.1, 127.3, 118.4, 118.2, 117.6, 18.2; HRMS (ESI) calcd for $C_{14}H_{11}N_2O_3$ (M - H^+) 255.0775, found 255.0771; Melting Point: 169–170 °C.

4.2.8. (E)-4-nitro-2-((m-tolylimino)methyl)phenol (5)

The title compound was prepared according to general procedure (**A**) using 5-nitrosalicylaldehyde (200 mg, 1.20 mmol) and 3-methylaniline **5a** (128 μL, 1.20 mmol, 1 equiv), yielding the pure product as a yellow solid (230 mg, 75%); ^{1}H NMR (400 MHz, Chloroform-*d*) δ 14.58 (s, 1H), 8.73 (s, 1H), 8.41 (d, J = 2.9 Hz, 1H), 8.28 (dd, J = 9.2, 2.8 Hz, 1H), 7.37 (t, J = 7.5 Hz, 1H), 7.21 – 7.15 (m, 3H), 7.11 (d, J = 9.3 Hz, 1H), 2.45 (s, 3H); ^{13}C NMR (100 MHz, Chloroform-*d*) δ 167.1, 160.3, 146.6, 139.9, 139.7, 129.5, 128.9, 128.4, 128.3, 121.9, 118.4, 118.2, 118.1, 21.4; HRMS (ESI) calcd for $C_{14}H_{11}N_2O_3$ (M - H^+) 255.0775, found 255.0772; Melting Point: 137–138 °C.

4.2.9. (E)-4-nitro-2-((p-tolylimino)methyl)phenol (6)

The title compound was prepared according to general procedure (**A**) using 5-nitrosalicylaldehyde (200 mg, 1.20 mmol) and 4-methylaniline **6a** (129 mg, 1.20 mmol, 1 equiv), yielding the pure product as a yellow solid (248 mg, 81%); ^{1}H NMR (400 MHz, Chloroform-*d*) δ 14.65 (s, 1H), 8.73 (s, 1H), 8.40 (d, J = 2.7 Hz, 1H), 8.28 (dd, J = 9.2, 2.8 Hz, 1H), 7.31 – 7.26 (m, 4H), 7.11 (d, J = 9.1 Hz, 1H), 2.43 (s, 3H); ^{13}C NMR (100 MHz, Chloroform-*d*) δ 167.0, 159.5, 143.9, 139.9, 138.4, 130.3, 128.2, 128.2, 121.1, 118.3, 118.2, 21.1; HRMS (ESI) calcd for $C_{14}H_{11}N_2O_3$ (M - H^+) 255.0775, found 255.0772; Melting Point: 160–161 °C.

4.2.10. (E)-2-(((3-(tert-butyl)phenyl)imino)methyl)-4-nitrophenol (7)

The title compound was prepared according to general procedure (**A**) using 5-nitrosalicylaldehyde (200 mg, 1.20 mmol) and 3-*tert*-butylbenzenamine **7a** (179 mg, 1.20 mmol, 1 equiv), yielding the pure product as a yellow solid (244 mg, 68%); ^{1}H NMR (400 MHz, Chloroform-*d*) δ 14.63 (s, 1H), 8.74 (s, 1H), 8.43 (d, J = 2.7 Hz, 1H), 8.29 (dd, J = 9.2, 2.6 Hz, 1H), 7.43 – 7.41 (m, 2H), 7.36 (d, J = 2.3 Hz, 1H), 7.19 – 7.15 (m, 1H), 7.12 (d, J = 9.2 Hz, 1H), 1.40 (s, 9H); ^{13}C NMR (100 MHz, Chloroform-*d*) δ 167.1, 160.3, 153.2, 146.5, 139.9, 129.4, 128.4, 128.3, 125.2, 118.8, 118.4, 118.1, 117.7, 34.9, 31.3; HRMS (ESI) calcd for $C_{17}H_{17}N_2O_3$ (M - H^+) 297.1245, found 297.1242; Melting Point: 128–129 °C.

4.2.11. (E)-2-(((2-methoxyphenyl)imino)methyl)-4-nitrophenol (8)

The title compound was prepared according to general procedure (**A**) using 5-nitrosalicylaldehyde (200 mg, 1.20 mmol) and 2-methoxyaniline **8a** (135 μL, 1.20 mmol, 1 equiv), yielding the pure product as a red solid (259 mg, 79%); ^{1}H NMR (400 MHz, Chloroform-*d*) δ 15.41 (s, 1H), 8.84 (s, 1H), 8.40 (d, J = 2.8 Hz, 1H), 8.26 (dd, J = 9.3, 2.8 Hz, 1H), 7.37 – 7.32 (m, 2H), 7.09 – 7.04 (m, 3H), 3.97 (s, 3H); ^{13}C NMR (100 MHz, Chloroform-*d*) δ 168.9, 159.4, 153.0, 139.2, 133.9, 129.3, 128.5, 128.3, 121.1, 119.7, 119.0, 117.8, 112.1, 55.9; HRMS (ESI) calcd for $C_{14}H_{11}N_2O_4$ (M - H^+) 271.0724, found 271.0719; Melting Point: 186–187 °C.

4.2.12. (E)-2-(((3-methoxyphenyl)imino)methyl)-4-nitrophenol (9)

The title compound was prepared according to general procedure (**A**) using 5-nitrosalicylaldehyde (200 mg, 1.20 mmol) and 3-methoxyaniline **9a** (136 μL, 1.20 mmol, 1 equiv), yielding the pure product as a yellow solid (264 mg, 81%); ^{1}H NMR (400 MHz, Chloroform-*d*) δ 14.43 (s, 1H), 8.73 (s, 1H), 8.42 (d, J = 2.7 Hz, 1H), 8.29 (dd, J = 9.1, 2.8 Hz, 1H), 7.39 (t, J = 8.1 Hz, 1H), 7.12 (d, J = 9.2 Hz, 1H), 6.96 – 6.92 (m, 2H), 6.88 (t, J = 2.2 Hz, 1H), 3.89 (s, 3H); ^{13}C NMR (100 MHz, Chloroform-*d*) δ 166.9, 160.8, 160.7, 148.0, 140.0, 130.5, 128.4, 128.4, 118.4, 118.1, 113.8, 113.3, 107.1, 55.5; HRMS (ESI) calcd for $C_{14}H_{11}N_2O_4$ (M - H^+) 271.0724, found 271.0721; Melting Point: 167–168 °C.

4.2.13. (E)-2-(((4-methoxyphenyl)imino)methyl)-4-nitrophenol (10)

The title compound was prepared according to general procedure (**A**) using 5-nitrosalicylaldehyde (200 mg, 1.20 mmol) and 4-methoxyaniline **10a** (148 mg, 1.20 mmol, 1 equiv), yielding the pure product as a yellow solid (268 mg, 82%); ^{1}H NMR (400 MHz, Chloroform-*d*) δ 14.70 (s, 1H), 8.71 (s, 1H), 8.39 (d, J = 2.8 Hz, 1H), 8.26 (dd, J = 9.1, 2.8 Hz, 1H), 7.38 – 7.34 (m, 2H), 7.10 (d, J = 9.2 Hz, 1H), 7.03 – 6.99 (m, 2H), 3.89 (s, 3H); ^{13}C NMR (100 MHz, Chloroform-*d*) δ 166.9, 159.8, 158.0, 139.9, 139.4, 128.0, 127.9, 122.5, 118.3, 118.2, 114.9, 55.6; HRMS (ESI) calcd for $C_{14}H_{11}N_2O_4$ (M - H^+) 271.0724, found 271.0727; Melting Point: 169–170 °C.

4.2.14. Methyl (E)-2-((2-hydroxy-5-nitrobenzylidene)amino)benzoate (11)

The title compound was prepared according to general procedure (**A**) using 5-nitrosalicylaldehyde (200 mg, 1.20 mmol) and methyl 2-aminobenzoate **11a** (155 μL, 1.20 mmol, 1 equiv), yielding the pure product as a red solid (285 mg, 79%); ^{1}H NMR (400 MHz, Chloroform-*d*) δ 14.29 (s, 1H), 8.66 (s, 1H), 8.43 (d, J = 2.7 Hz, 1H), 8.30 (dd, J = 9.2, 2.8 Hz, 1H), 8.09 (dd, J = 7.9, 1.6 Hz, 1H), 7.66 (td, J = 7.7, 1.6 Hz, 1H), 7.44 (td, J = 7.6, 1.1 Hz, 1H), 7.26 (dd, J = 8.0, 1.1 Hz, 1H), 7.14 (d, J = 9.3 Hz, 1H), 3.96 (s, 3H); ^{13}C NMR (100 MHz, Chloroform-*d*) δ 166.9, 166.3, 161.0, 147.3, 139.8, 133.7, 131.7, 128.6, 128.6, 127.4, 124.4, 119.1, 118.7, 118.3, 52.4; HRMS (ESI) calcd for $C_{15}H_{11}N_2O_5$ (M - H^+) 299.0673, found 299.0672; Melting Point: 176–177 °C.

4.2.15. Methyl (E)-3-((2-hydroxy-5-nitrobenzylidene)amino)benzoate (12)

The title compound was prepared according to general procedure (**A**) using 5-nitrosalicylaldehyde (200 mg, 1.20 mmol) and methyl 3-aminobenzoate **12a** (181 mg, 1.20 mmol, 1 equiv), yielding the pure product as a yellow solid (307 mg, 85%); ^{1}H NMR (400 MHz, Chloroform-*d*) δ 14.12 (s, 1H), 8.80 (s, 1H), 8.45 (d, J = 2.8 Hz, 1H), 8.32 (dd, J = 9.1, 2.8 Hz, 1H), 8.07 – 8.02 (m, 2H), 7.60 – 7.53 (m, 2H), 7.15 (d, J = 9.2 Hz, 1H), 3.99 (s, 3H); ^{13}C NMR (100 MHz, DMSO-d_6) δ 166.6, 166.2, 162.8, 147.9, 139.8, 131.4, 130.5, 129.0, 128.6, 128.4, 127.0, 122.1, 119.4, 118.5, 52.8; HRMS (ESI) calcd for $C_{15}H_{11}N_2O_5$ (M - H^+) 299.0673, found 299.0669; Melting Point: 201–202 °C.

4.2.16. Methyl (E)-4-((2-hydroxy-5-nitrobenzylidene)amino)benzoate (13)

The title compound was prepared according to general procedure (**A**) using 5-nitrosalicylaldehyde (200 mg, 1.20 mmol) and methyl 4-aminobenzoate **13a** (181 mg, 1.20 mmol, 1 equiv), yielding the pure product as a yellow solid (294 mg, 82%); ^{1}H NMR (400 MHz, Chloroform-*d*) δ 13.99 (s, 1H), 8.76 (s, 1H), 8.45 (d, J = 2.8 Hz, 1H), 8.32 (dd, J = 9.2, 2.7 Hz, 1H), 8.18 – 8.16 (m, 2H), 7.40 – 7.38 (m, 2H), 7.15 (d, J = 9.1 Hz, 1H), 3.98 (s, 3H); ^{13}C NMR (100 MHz, Chloroform-*d*) δ 166.6, 166.3, 162.4, 150.8, 140.2, 131.3, 129.5, 128.9, 128.7, 121.2, 118.5, 118.0, 52.3; HRMS (ESI) calcd for $C_{15}H_{11}N_2O_5$ (M - H^+) 299.0673, found 299.0672; Melting Point: 206–207 °C.

4.2.17. (E)-2-(((3-ethynylphenyl)imino)methyl)-4-nitrophenol (14)

The title compound was prepared according to general procedure (**A**) using 5-nitrosalicylaldehyde (200 mg, 1.20 mmol) and 3-aminophenylacetylene **14a** (135 μL, 1.20 mmol, 1 equiv), yielding the pure product as a yellow solid (242 mg, 76%); ^{1}H NMR (400 MHz, DMSO-d_6) δ 13.94 (br s, 1H), 9.16 (s, 1H), 8.66 (d, J = 2.8 Hz, 1H), 8.27 (dd, J = 9.3, 2.9 Hz, 1H), 7.59 – 7.44 (m, 4H), 7.13 (d, J = 9.2 Hz, 1H), 4.29 (s, 1H); ^{13}C NMR (100 MHz, DMSO-d_6) δ 166.8, 162.8, 147.8, 139.8,

131.1, 130.4, 128.9, 128.7, 124.6, 123.4, 123.1, 119.3, 118.6, 83.3, 81.9; HRMS (ESI) calcd for $C_{15}H_9N_2O_3$ (M - H^+) 265.0619, found 265.0620; Melting Point: 196–197 °C.

4.2.18. (E)-2-(((3-(hydroxymethyl)phenyl)imino)methyl)-4-nitrophenol (15)

The title compound was prepared according to general procedure (**A**) using 5-nitrosalicylaldehyde (200 mg, 1.20 mmol) and 3-aminobenzyl alcohol **15a** (148 mg, 1.20 mmol, 1 equiv), yielding the pure product as a yellow solid (277 mg, 85%); ^{1}H NMR (400 MHz, DMSO-d_6) δ 14.52 (br s, 1H), 9.21 (s, 1H), 8.71 (d, J = 2.9 Hz, 1H), 8.26 (dd, J = 9.3, 2.9 Hz, 1H), 7.48 – 7.44 (m, 2H), 7.38 – 7.31 (m, 2H), 7.11 (d, J = 9.1 Hz, 1H), 5.34 (t, J = 5.8 Hz, 1H), 4.58 (d, J = 3.9 Hz, 2H); ^{13}C NMR (100 MHz, DMSO-d_6) δ 167.9, 161.8, 146.5, 144.8, 139.4, 129.8, 129.0, 128.9, 126.2, 120.1, 119.7, 119.0, 63.0; HRMS (ESI) calcd for $C_{14}H_{11}N_2O_4$ (M - H^+) 271.0724, found 271.0721; Melting Point: 170–171 °C.

4.2.19. (E)-2-(((4-(hydroxymethyl)phenyl)imino)methyl)-4-nitrophenol (16)

The title compound was prepared according to general procedure (**A**) using 5-nitrosalicylaldehyde (200 mg, 1.20 mmol) and 4-aminobenzyl alcohol **16a** (148 mg, 1.20 mmol, 1 equiv), yielding the pure product as a yellow solid (293 mg, 90%); ^{1}H NMR (400 MHz, DMSO-d_6) δ 14.58 (br s, 1H), 9.20 (s, 1H), 8.66 (d, J = 3.0 Hz, 1H), 8.25 (dd, J = 9.3, 2.9 Hz, 1H), 7.48 – 7.43 (m, 4H), 7.10 (d, J = 9.3 Hz, 1H), 5.29 (br s, 1H), 4.55 (s, 2H); ^{13}C NMR (100 MHz, DMSO-d_6) δ 167.8, 161.5, 145.1, 142.9, 139.4, 129.0, 128.8, 128.0, 121.6, 118.9, 118.9, 62.9; HRMS (ESI) calcd for $C_{14}H_{11}N_2O_4$ (M - H^+) 271.0724, found 271.0722; Melting Point: 184–185 °C.

4.2.20. 2-(((2-fluorophenyl)amino)methyl)-4-nitrophenol (17)

The title compound was prepared according to general procedure (**B**) using **1** (100 mg, 0.38 mmol), yielding the pure product as a yellow solid (92 mg, 91%) after flash chromatography (Hexane : EtOAc = 15 : 1); ^{1}H NMR (400 MHz, Chloroform-*d*) δ 9.57 (br s, 1H), 8.17 – 8.15 (m, 2H), 7.12 – 7.05 (m, 2H), 6.98 – 6.89 (m, 3H), 4.57 (s, 2H), 4.42 (s, 1H); ^{13}C NMR (100 MHz, Chloroform-*d*) δ 162.8, 153.1 (d, J = 242.4 Hz), 140.9, 134.6 (d, J = 12.1 Hz), 125.5, 124.9 (d, J = 4.0 Hz), 124.7, 123.1, 121.7 (d, J = 8.1 Hz), 117.1, 116.1 (d, J = 3.0 Hz), 115.2 (d, J = 19.2 Hz), 48.3; HRMS (ESI) calcd for $C_{13}H_{10}FN_2O_3$ (M - H^+) 261.0681, found 261.0683; Melting Point: 107–108 °C.

4.2.21. 2-(((3-fluorophenyl)amino)methyl)-4-nitrophenol (18)

The title compound was prepared according to general procedure (**B**) using **2** (100 mg, 0.38 mmol), yielding the pure product as a yellow solid (90 mg, 89%) after flash chromatography (Hexane : EtOAc = 15 : 1); ^{1}H NMR (400 MHz, Chloroform-*d*) δ 9.37 (br s, 1H), 8.16 – 8.14 (m, 2H), 7.22 (q, J = 7.7 Hz, 1H), 6.97 – 6.95 (m, 1H), 6.69 – 6.63 (m, 2H), 6.58 – 6.55 (m, 1H), 4.53 (s, 2H), 4.28 (br s, 1H); ^{13}C NMR (100 MHz, DMSO-d_6) δ 163.9 (d, J = 240.4 Hz), 162.1, 150.9 (d, J = 11.1 Hz), 140.1, 130.8 (d, J = 11.1 Hz), 127.5, 124.9, 124.3, 115.6, 108.9 (d, J = 2.0 Hz), 102.6 (d, J = 21.2 Hz), 98.8 (d, J = 25.3 Hz), 41.1; HRMS (ESI) calcd for $C_{13}H_{10}FN_2O_3$ (M - H^+) 261.0681, found 261.0679; Melting Point: 122–123 °C.

4.2.22. 2-(((4-fluorophenyl)amino)methyl)-4-nitrophenol (19)

The title compound was prepared according to general procedure (**B**) using **3** (100 mg, 0.38 mmol), yielding the pure product as a yellow solid (94 mg, 93%) after flash chromatography (Hexane : EtOAc = 15 : 1); ^{1}H NMR (400 MHz, Chloroform-*d*) δ 10.20 (br s, 1H), 8.15 (dd, J = 8.8, 2.8 Hz, 1H), 8.12 (d, J = 2.8 Hz, 1H), 7.02 – 6.97 (m, 2H), 6.95 (d, J = 8.8 Hz, 1H), 6.85 (dd, J = 9.0, 4.4 Hz, 2H), 4.53 (s, 2H), 4.07 (s, 1H); ^{13}C NMR (100 MHz, Chloroform-*d*) δ 163.3, 158.4 (d, J = 242.4 Hz), 142.1 (d, J = 2.0 Hz), 140.8, 125.5, 124.5, 122.7, 118.0 (d, J = 8.1 Hz), 117.2, 116.2 (d, J = 23.2 Hz), 49.7; HRMS (ESI) calcd for $C_{13}H_{10}FN_2O_3$ (M - H^+) 261.0681, found 261.0682; Melting Point: 131–132 °C.

4.2.23. 4-nitro-2-((o-tolylamino)methyl)phenol (20)

The title compound was prepared according to general procedure (**B**) using **4** (100 mg, 0.39 mmol), yielding the pure product as a yellow solid (93 mg, 92%) after flash chromatography (Hexane : EtOAc = 15 : 1); ^{1}H NMR (400 MHz, Chloroform-*d*) δ 10.10 (br s, 1H), 8.17 – 8.15 (m, 2H), 7.22 – 7.18 (m, 2H), 6.98 – 6.94 (m, 2H), 6.88 (d, J = 8.1 Hz, 1H), 4.59 (s, 2H), 3.95 (br s, 1H), 2.29 (s, 3H); ^{13}C NMR (100 MHz, Chloroform-*d*) δ 163.3, 143.9, 140.8, 130.7, 127.4, 125.9, 125.4, 124.7, 123.0, 121.8, 117.1, 114.1, 48.5, 17.6; HRMS (ESI) calcd for $C_{14}H_{13}N_2O_3$ (M - H^+) 257.0932, found 257.0928; Melting Point: 105–106 °C.

4.2.24. 4-nitro-2-((m-tolylamino)methyl)phenol (21)

The title compound was prepared according to general procedure (**B**) using **5** (100 mg, 0.39 mmol), yielding the pure product as a yellow solid (95 mg, 94%) after flash chromatography (Hexane : EtOAc = 15 : 1); ^{1}H NMR (400 MHz, Chloroform-*d*) δ 8.14 (d, J = 10.1 Hz, 2H), 7.18 (t, J = 7.6 Hz, 1H), 6.95 (d, J = 8.8 Hz, 1H), 6.84 (d, J = 7.6 Hz, 1H), 6.71 (d, J = 5.5 Hz, 2H), 4.54 (s, 2H), 2.33 (s, 3H); ^{13}C NMR (100 MHz, Chloroform-*d*) δ 163.4, 146.0, 140.8, 139.6, 129.4, 125.4, 124.5, 123.0, 123.0, 117.5, 117.1, 113.6, 49.2, 21.5; HRMS (ESI) calcd for $C_{14}H_{13}N_2O_3$ (M - H^+) 257.0932, found 257.0928; Melting Point: 140–141 °C.

4.2.25. 4-nitro-2-((p-tolylamino)methyl)phenol (22)

The title compound was prepared according to general procedure (**B**) using **6** (100 mg, 0.39 mmol), yielding the pure product as a yellow solid (94 mg, 93%) after flash chromatography (Hexane : EtOAc = 15 : 1); ^{1}H NMR (400 MHz, Chloroform-*d*) δ 10.49 (br s, 1H), 8.17 – 8.12 (m, 2H), 7.10 (d, J = 8.3 Hz, 2H), 6.94 (d, J = 8.8 Hz, 1H), 6.81 (d, J = 8.4 Hz, 2H), 4.54 (s, 2H), 4.02 (br s, 1H), 2.31 (s, 3H); ^{13}C NMR (100 MHz, Chloroform-*d*) δ 163.5, 143.4, 140.7, 131.8, 130.1, 125.4, 124.5, 122.9, 117.1, 116.9, 49.7, 20.6; HRMS (ESI) calcd for $C_{14}H_{13}N_2O_3$ (M - H^+) 257.0932, found 257.0927; Melting Point: 118–119 °C.

4.2.26. 2-(((3-(tert-butyl)phenyl)amino)methyl)-4-nitrophenol (23)

The title compound was prepared according to general procedure (**B**) using **7** (100 mg, 0.34 mmol), yielding the pure product as a yellow solid (94 mg, 93%) after flash chromatography (Hexane : EtOAc = 15 : 1); ^{1}H NMR (400 MHz, Chloroform-*d*) δ 10.30 (br s, 1H), 8.17 – 8.15 (m, 2H), 7.24 (t, J = 8.0 Hz, 1H), 7.06 (d, J = 7.9 Hz, 1H), 6.97 – 6.92 (m, 2H), 6.72 (d, J = 8.1 Hz, 1H), 4.57 (s, 2H), 4.08 (s, 1H), 1.30 (s, 9H); ^{13}C NMR (100 MHz, Chloroform-*d*) δ 163.4, 152.9, 145.8, 140.7, 129.3, 125.4, 124.5, 123.1, 119.4, 117.1, 114.3, 113.4, 49.4, 34.7, 31.2; HRMS (ESI) calcd for $C_{17}H_{19}N_2O_3$ (M - H^+) 299.1401, found 299.1399; Melting Point: 112–113 °C.

4.2.27. 2-(((2-methoxyphenyl)amino)methyl)-4-nitrophenol (24)

The title compound was prepared according to general procedure (**B**) using **8** (100 mg, 0.36 mmol), yielding the pure product as a yellow solid (88 mg, 87%) after flash chromatography (Hexane : EtOAc = 10 : 1); ^{1}H NMR (400 MHz, Chloroform-*d*) δ 10.39 (br s, 1H), 8.20 – 8.11 (m, 2H), 7.02 – 6.80 (m, 5H), 4.70 (br s, 1H), 4.54 (s, 2H), 3.90 (s, 3H); ^{13}C NMR (100 MHz, Chloroform-*d*) δ 163.5, 148.9, 140.7, 135.8, 125.3, 124.4, 123.3, 121.7, 121.2, 117.1, 114.8, 110.1, 55.6, 49.1; HRMS (ESI) calcd for $C_{14}H_{13}N_2O_4$ (M - H^+) 273.0881, found 273.0878; Melting Point: 124–125 °C.

4.2.28. 2-(((3-methoxyphenyl)amino)methyl)-4-nitrophenol (25)

The title compound was prepared according to general procedure (**B**) using **9** (100 mg, 0.37 mmol), yielding the pure product as a yellow solid (90 mg, 89%) after flash chromatography (Hexane : EtOAc = 15 :

1); ^{1}H NMR (400 MHz, Chloroform-*d*) δ 9.93 (br s, 1H), 8.17 – 8.14 (m, 2H), 7.20 (t, J = 8.1 Hz, 1H), 6.95 (d, J = 8.6 Hz, 1H), 6.56 (dd, J = 8.2, 2.4 Hz, 1H), 6.48 (dd, J = 7.9, 2.3 Hz, 1H), 6.43 (d, J = 2.4 Hz, 1H), 4.54 (s, 2H), 3.79 (s, 3H); ^{13}C NMR (100 MHz, Chloroform-*d*) δ 163.1, 160.7, 147.6, 140.8, 130.4, 125.4, 124.5, 123.1, 117.0, 109.0, 106.8, 102.8, 55.2, 48.7; HRMS (ESI) calcd for $C_{14}H_{13}N_2O_4$ (M - H^+) 273.0881, found 273.0876; Melting Point: 98–99 °C.

4.2.29. 2-(((4-methoxyphenyl)amino)methyl)-4-nitrophenol (26)

The title compound was prepared according to general procedure (**B**) using **10** (100 mg, 0.37 mmol), yielding the pure product as a yellow solid (87 mg, 86%) after flash chromatography (Hexane : EtOAc = 10 : 1); ^{1}H NMR (400 MHz, DMSO-d_6) δ 8.09 (d, J = 2.9 Hz, 1H), 8.02 (dd, J = 9.0, 3.0 Hz, 1H), 6.99 (d, J = 8.9 Hz, 1H), 6.70 (d, J = 8.4 Hz, 2H), 6.51 (d, J = 8.5 Hz, 2H), 4.20 (s, 2H), 3.62 (s, 3H); ^{13}C NMR (100 MHz, DMSO-d_6) δ 162.1, 151.4, 142.9, 140.1, 128.4, 124.6, 124.2, 115.5, 115.1, 113.7, 55.7, 42.1; HRMS (ESI) calcd for $C_{14}H_{13}N_2O_4$ (M - H^+) 273.0881, found 273.0881; Melting Point: 140–141 °C.

4.2.30. Methyl 2-((2-hydroxy-5-nitrobenzyl)amino)benzoate (27)

The title compound was prepared according to general procedure (**B**) using **11** (100 mg, 0.33 mmol), yielding the pure product as a yellow solid (90 mg, 89%) after flash chromatography (Hexane : EtOAc = 15 : 1); ^{1}H NMR (400 MHz, Chloroform-*d*) δ 8.65 (br s, 1H), 8.18 (d, J = 2.8 Hz, 1H), 8.14 (dd, J = 8.8, 2.8 Hz, 1H), 8.04 (br s, 1H), 8.01 (dd, J = 7.9, 1.7 Hz, 1H), 7.42 (ddd, J = 8.5, 7.3, 1.7 Hz, 1H), 6.94 (d, J = 8.8 Hz, 1H), 6.89 – 6.82 (m, 2H), 4.60 (d, J = 4.9 Hz, 2H), 3.92 (s, 3H); ^{13}C NMR (100 MHz, DMSO-d_6) δ 168.5, 162.6, 150.7, 139.8, 135.3, 131.7, 127.0, 125.2, 124.4, 115.8, 115.4, 112.1, 110.1, 52.1, 41.2; HRMS (ESI) calcd for $C_{15}H_{13}N_2O_5$ (M - H^+) 301.0830, found 301.0833; Melting Point: 175–176 °C.

4.2.31. Methyl 3-((2-hydroxy-5-nitrobenzyl)amino)benzoate (28)

The title compound was prepared according to general procedure (**B**) using **12** (100 mg, 0.33 mmol), yielding the pure product as a yellow solid (88 mg, 87%) after flash chromatography (Hexane : EtOAc = 10 : 1); ^{1}H NMR (400 MHz, DMSO-d_6) δ 11.36 (br s, 1H), 8.08 – 8.02 (m, 2H), 7.22 – 7.14 (m, 3H), 7.02 (d, J = 8.9 Hz, 1H), 6.82 (d, J = 8.1 Hz, 1H), 6.63 (br s, 1H), 4.29 (s, 2H), 3.79 (s, 3H); ^{13}C NMR (100 MHz, DMSO-d_6) δ 167.1, 162.1, 149.0, 140.1, 130.8, 129.8, 127.5, 124.9, 124.1, 117.3, 117.0, 115.6, 112.9, 52.4, 41.1; HRMS (ESI) calcd for $C_{15}H_{13}N_2O_5$ (M - H^+) 301.0830, found 301.0831; Melting Point: 130–131 °C.

4.2.32. Methyl 4-((2-hydroxy-5-nitrobenzyl)amino)benzoate (29)

The title compound was prepared according to general procedure (**B**) using **13** (100 mg, 0.33 mmol), yielding the pure product as a yellow solid (87 mg, 86%) after flash chromatography (Hexane : EtOAc = 15 : 1); ^{1}H NMR (400 MHz, DMSO-d_6) δ 11.38 (br s, 1H), 8.05 (d, J = 7.8 Hz, 2H), 7.69 (d, J = 8.5 Hz, 2H), 7.11 (t, J = 6.0 Hz, 1H), 7.02 (d, J = 8.1 Hz, 1H), 6.62 (d, J = 8.6 Hz, 2H), 4.33 (d, J = 5.9 Hz, 2H), 3.74 (s, 3H); ^{13}C NMR (100 MHz, DMSO-d_6) δ 166.7, 162.1, 152.9, 140.0, 131.5, 127.1, 125.0, 124.2, 116.9, 115.7, 111.7, 51.7, 40.8; HRMS (ESI) calcd for $C_{15}H_{13}N_2O_5$ (M - H^+) 301.0830, found 301.0826; Melting Point: 203–204 °C.

4.2.33. 2-(((3-ethynylphenyl)amino)methyl)-4-nitrophenol (30)

The title compound was prepared according to general procedure (**B**) using **14** (100 mg, 0.38 mmol), yielding the pure product as a yellow solid (93 mg, 92%) after flash chromatography (Hexane : EtOAc = 15 : 1); ^{1}H NMR (400 MHz, Chloroform-*d*) δ 9.58 (br s, 1H), 8.16 – 8.14 (m, 2H), 7.24 (t, J = 7.9 Hz, 1H), 7.13 (d, J = 7.8 Hz, 1H), 7.00 – 6.95 (m, 2H), 6.86 (d, J = 8.2 Hz, 1H), 4.54 (s, 2H), 4.16 (s, 1H), 3.09 (s, 1H); ^{13}C NMR (100 MHz, Chloroform-*d*) δ 162.81, 146.12, 140.93, 129.59, 125.66, 125.53, 124.63, 123.34, 122.81, 119.54, 117.14, 116.90, 83.21, 77.59, 48.46; HRMS (ESI) calcd for $C_{15}H_{11}N_2O_3$ (M - H^+) 267.0775, found 267.0773; Melting point: 134–135 °C.

4.2.34. 2-(((3-(hydroxymethyl)phenyl)amino)methyl)-4-nitrophenol (31)

The title compound was prepared according to general procedure (**B**) using **15** (100 mg, 0.38 mmol), yielding the pure product as a yellow solid (85 mg, 84%) after flash chromatography (Hexane : EtOAc = 15 : 1); ^{1}H NMR (400 MHz, DMSO-d_6) δ 11.29 (br s, 1H), 8.09 (d, J = 2.9 Hz, 1H), 8.03 (dd, J = 9.0, 2.9 Hz, 1H), 7.02 – 6.98 (m, 2H), 6.59 – 6.49 (m, 2H), 6.41 (dd, J = 7.9, 2.3 Hz, 1H), 5.01 (br s, 1H), 4.36 (s, 2H), 4.25 (s, 2H); ^{13}C NMR (100 MHz, DMSO-d_6) δ 162.0, 148.7, 143.8, 140.1, 129.1, 128.3, 124.7, 124.0, 115.5, 114.9, 110.9, 110.8, 63.7, 41.3; HRMS (ESI) calcd for $C_{14}H_{13}N_2O_4$ (M - H^+) 273.0881, found 273.0879; Melting Point: 136–137 °C.

4.2.35. 5-nitro-2-((2-(trimethylsilyl)ethoxy)methoxy)benzaldehyde (32a)

To a mixture of 5-nitrosalicylaldehyde (500 mg, 2.99 mmol) and DIPEA (1.24 mL, 7.48 mmol, 2.5 equiv) in dry DCM (30 mL) was added 2-(trimethylsilyl)ethoxymethyl chloride (530 µL, 2.99 mmol, 1 equiv), and the reaction mixture was stirred at room temperature until complete consumption of the starting material as determined by TLC. The product was extracted with EtOAc (20 mL × 3). The organic layers were combined, washed with saturated brine, dried over Na_2SO_4 and filtered. All volatiles were evaporated *in vacuo* and the product was obtained after flash chromatography (Hexane : EtOAc = 30: 1) as a light yellow liquid (716 mg, 80%); ^{1}H NMR (400 MHz, Chloroform-*d*) δ 10.49 (s, 1H), 8.73 (d, J = 2.9 Hz, 1H), 8.42 (dd, J = 9.3, 2.9 Hz, 1H), 7.42 (d, J = 9.3 Hz, 1H), 5.48 (s, 2H), 3.85 (t, J = 8.2 Hz, 2H), 1.00 (t, J = 8.2 Hz, 2H), 0.03 (s, 9H).

4.2.36. (E)-4-nitro-2-styrylphenol (32)

Step 1: (E)-trimethyl(2-((4-nitro-2-styrylphenoxy)methoxy)ethyl)silane (**32b**). To a solution of diethyl benzylphosphonate (171 µL, 0.84 mmol, 1 equiv) in dry THF (10 mL) at 0 °C was added NaH (40 mg, 60% in mineral oil, 1.00 mmol, 1.2 equiv). The resulting mixture was stirred at the same temperature for 30 min and **32a** (250 mg, 0.84 mmol) in dry THF (5 mL) was added dropwisely. The mixture was stirred at room temperature overnight before extracted with EtOAc (20 mL × 3). The organic layers were combined, washed with saturated brine, dried over Na_2SO_4 and filtered. All volatiles were evaporated *in vacuo* and the crude product was used directly in the next step without further purification.

Step 2: Crude **32b** obtained in last step was dissolved in 2% H_2SO_4-methanol solution (10 mL). The mixture was stirred at room temperature for 3 h, then quenched with water and the product was extracted with EtOAc (20 mL × 3). The organic layers were combined, washed with saturated brine, dried over Na_2SO_4 and filtered. All volatiles were evaporated *in vacuo* and the product was obtained after flash chromatography (Hexane : EtOAc = 10 : 1) as a yellow solid (71 mg, 35% in two steps); ^{1}H NMR (400 MHz, DMSO-d_6) δ 11.48 (br s, 1H), 8.48 (d, J = 2.8 Hz, 1H), 8.05 (d, J = 9.0 Hz, 1H), 7.64 – 7.62 (m, 2H), 7.47 (d, J = 16.5 Hz, 1H), 7.42 – 7.38 (m, 3H), 7.30 (t, J = 7.3 Hz, 1H), 7.06 (d, J = 8.9 Hz, 1H); ^{13}C NMR (100 MHz, Chloroform-*d*) δ 158.38, 141.90, 136.62, 132.76, 128.83, 128.46, 126.87, 125.66, 124.24, 122.96, 120.60, 116.09; HRMS (ESI) calcd for $C_{14}H_{10}NO_3$ (M - H^+) 240.0666, found 240.0662; Melting point: 136–137 °C.

4.2.37. Trimethyl(2-((4-nitro-2-vinylphenoxy)methoxy)ethyl)silane (33a)

To a solution of methyltriphenylphosphonium bromide (3.6 g, 10.08 mmol, 1.5 equiv) in dry THF (30 mL) at 0 °C was added NaH (444 mg, 60% in mineral oil, 11.1 mmol, 1.65 equiv). The resulting mixture was stirred at the same temperature for 30 min and **32a** (2 g, 6.73 mmol) in dry THF (10 mL) was added dropwisely via syringe under N2 atmosphere. The mixture was stirred at room temperature overnight

before extracted with EtOAc (20 mL × 3). The organic layers were combined, washed with saturated brine, dried over Na_2SO_4 and filtered. All volatiles were evaporated *in vacuo* and the product was obtained after flash chromatography (Hexane : EtOAc = 100 : 1) as a white solid (1238 mg, 62%); ^{1}H NMR (400 MHz, Chloroform-*d*) δ 8.40 (d, J = 2.8 Hz, 1H), 8.13 (dd, J = 9.2, 2.9 Hz, 1H), 7.23 (d, J = 9.1 Hz, 1H), 7.04 (dd, J = 17.7, 11.1 Hz, 1H), 6.15 – 5.72 (m, 1H), 5.60 – 5.42 (m, 1H), 5.38 (s, 2H), 3.83 – 3.76 (m, 2H), 1.03 – 0.93 (m, 2H), 0.02 (s, 9H).

4.2.38. (E)-2-(2-methoxystyryl)-4-nitrophenol (33)

The title compound was prepared according to general procedure (**D**) using 2-iodoanisole **33b** (73 µL, 0.56 mmol), yielding the pure product as a yellow solid (97 mg, 64%) after flash chromatography (Hexane : EtOAc = 20 : 1); ^{1}H NMR (400 MHz, Chloroform-*d*) δ 8.49 (d, J = 2.7 Hz, 1H), 8.06 (dd, J = 9.0, 2.8 Hz, 1H), 7.63 (d, J = 7.8 Hz, 1H), 7.59 (d, J = 16.6 Hz, 1H), 7.34 – 7.28 (m, 2H), 7.01 (t, J = 7.5 Hz, 1H), 6.94 (dd, J = 14.9, 8.6 Hz, 2H), 6.03 (s, 1H), 3.94 (s, 3H); ^{13}C NMR (10 MHz, DMSO-d_6) δ 161.5, 157.2, 140.4, 129.8, 127.0, 126.0, 125.9, 125.6, 124.7, 122.7, 122.7, 121.2, 116.5, 111.9, 56.0; HRMS (ESI) calcd for $C_{15}H_{12}NO_4$ (M - H^+) 270.0772, found 270.0769; Melting point: 183–184 °C.

4.2.39. (E)-2-(3-methoxystyryl)-4-nitrophenol (34)

The title compound was prepared according to general procedure (**D**) using 3-iodoanisole **34b** (67 µL, 0.56 mmol), yielding the pure product as a yellow solid (89 mg, 58%) after flash chromatography (Hexane : EtOAc = 20 : 1); ^{1}H NMR (400 MHz, Chloroform-*d*) δ 8.48 (d, J = 2.8 Hz, 1H), 8.08 (dd, J = 8.9, 2.7 Hz, 1H), 7.39 – 7.29 (m, 2H), 7.23 (d, J = 16.4 Hz, 1H), 7.18 (d, J = 7.6 Hz, 1H), 7.11 (t, J = 2.2 Hz, 1H), 6.93 – 6.89 (m, 2H), 6.13 (s, 1H), 3.89 (s, 3H); ^{13}C NMR (100 MHz, DMSO-d_6) δ 161.6, 160.1, 140.5, 138.9, 131.3, 130.2, 125.1, 124.9, 123.0, 122.5, 119.5, 116.6, 114.3, 112.2, 55.5; HRMS (ESI) calcd for $C_{15}H_{12}NO_4$ (M - H^+) 270.0772, found 270.0771; Melting point: 158–159 °C.

4.2.40. (E)-2-(2-hydroxy-5-nitrostyryl)benzonitrile (35)

The title compound was prepared according to general procedure (**D**) using 2-iodobenzonitrile **35b** (128 mg, 0.56 mmol), yielding the pure product as a yellow solid (95 mg, 64%) after flash chromatography (Hexane : EtOAc = 20 : 1); ^{1}H NMR (400 MHz, DMSO-d_6) δ 11.82 (s, 1H), 8.45 (s, 1H), 8.11 – 8.02 (m, 2H), 7.87 – 7.46 (m, 3H), 7.66 – 7.49 (m, 2H), 7.08 (d, J = 9.1 Hz, 1H); ^{13}C NMR (100 MHz, DMSO-d_6) δ 162.3, 140.6, 140.4, 133.9, 133.7, 128.9, 128.5, 127.1, 126.2, 125.8, 125.0, 124.0, 118.3, 116.9, 110.7; HRMS (ESI) calcd for $C_{15}H_9N_2O_3$ (M - H^+) 265.0619, found 265.0617; Melting point: 216–217 °C.

4.2.41. Methyl (E)-3-(2-hydroxy-5-nitrostyryl)benzoate (36)

The title compound was prepared according to general procedure (**D**) using methyl 3-iodobenzoate **36b** (147 mg, 0.56 mmol), yielding the pure product as a yellow solid (102 mg, 61%) after flash chromatography (Hexane : EtOAc = 20 : 1); ^{1}H NMR (400 MHz, DMSO-d_6) δ 11.53 (br s, 1H), 8.53 (d, J = 2.9 Hz, 1H), 8.19 (s, 1H), 8.06 (dd, J = 9.0, 2.9 Hz, 1H), 7.92 (d, J = 7.9 Hz, 1H), 7.88 (d, J = 7.7 Hz, 1H), 7.61 – 7.53 (m, 2H), 7.48 (d, J = 16.6 Hz, 1H), 7.07 (d, J = 9.0 Hz, 1H), 3.89 (s, 3H); ^{13}C NMR (100 MHz, DMSO-d_6) δ 166.6, 161.6, 140.5, 138.0, 131.5, 130.6, 130.1, 129.7, 128.8, 127.5, 125.1, 124.8, 123.3, 123.0, 116.6, 52.7; HRMS (ESI) calcd for $C_{16}H_{12}NO_5$ (M - H^+) 298.0721, found 298.0717; Melting point: 200–201 °C.

4.2.42. Methyl (E)-4-(2-hydroxy-5-nitrostyryl)benzoate (37)

The title compound was prepared according to general procedure (**D**) using methyl 4-iodobenzoate **37b** (147 mg, 0.56 mmol), yielding the pure product as a yellow solid (113 mg, 67%) after flash chromatography (Hexane : EtOAc = 20 : 1); ^{1}H NMR (400 MHz, DMSO-d_6) δ 11.60 (br s, 1H), 8.52 (d, J = 2.7 Hz, 1H), 8.07 (dd, J = 9.0, 2.8 Hz, 1H), 7.97 (d, J = 8.1 Hz, 2H), 7.77 (d, J = 8.1 Hz, 2H), 7.55 (s, 2H), 7.07 (d, J = 9.0 Hz, 1H), 3.86 (s, 3H); ^{13}C NMR (100 MHz, DMSO-d_6) δ 166.4, 161.8, 142.2, 140.5, 130.1, 129.0, 127.2, 125.4, 124.9, 124.6, 123.3, 116.7, 52.5; HRMS (ESI) calcd for $C_{16}H_{12}NO_5$ (M - H^+) 298.0721, found 298.0719; Melting point: 258–259 °C.

4.2.43. N-(3-ethynylphenyl)-2-hydroxy-5-nitrobenzamide (38)

To a solution a of 5-nitrosalicylic acid (50 mg, 0.27 mmol) and triphenyl phosphite (86 µL, 0.33 mmol, 1.2 equiv) in toluene (5 mL) was added 3-aminophenylacetylene (37 µL, 0.33 mmol, 1.2 equiv) in toluene (2 mL) via syringe under N_2 atmosphere. The resulting mixture was refluxed for 6 h. After the reaction was completed, the product was extracted with EtOAc (20 mL × 3). The organic layers were combined, washed with saturated brine, dried over Na_2SO_4 and filtered. All volatiles were evaporated *in vacuo* and the product was obtained after flash chromatography (Hexane : EtOAc = 20 : 1) as a yellow solid (57 mg, 74%); ^{1}H NMR (400 MHz, DMSO-d_6) δ 10.64 (s, 1H), 8.74 (d, J = 3.0 Hz, 1H), 8.30 (dd, J = 9.1, 3.0 Hz, 1H), 7.91 (s, 1H), 7.74 – 7.72 (m, 1H), 7.41 (t, J = 7.9 Hz, 1H), 7.27 (d, J = 7.6 Hz, 1H), 7.17 (d, J = 9.1 Hz, 1H), 4.23 (s, 1H); ^{13}C NMR (100 MHz, DMSO-d_6) δ 164.7, 163.6, 139.8, 138.7, 129.7, 128.9, 128.0, 126.3, 124.0, 122.6, 121.8, 120.0, 118.5, 83.7, 81.2; HRMS (ESI) calcd for $C_{15}H_9N_2O_4$ (M - H^+) 281.0568, found 281.0571;. 181 °C (decomposed).

4.2.44. (2-hydroxy-5-nitrophenyl)(phenyl)methanone (39)

To a solution of 5-nitrosalicylaldehyde (100 mg, 0.60 mmol), $PdCl_2$ (5 mg, 0.03 mmol, 0.05 equiv), LiCl (5 mg, 0.12 mmol, 0.2 equiv) and Na_2CO_3 (127 mg, 1.20 mmol, 2equiv) in DMF (5 mL) was added iodobenzene (135 µL, 1.2 mmol, 2equiv) via syringe under N_2 atmosphere. The resulting solution was stirred at 120 °C for 6 h. After the reaction was completed, the product was extracted with EtOAc (20 mL × 3). The organic layers were combined, washed with saturated brine, dried over Na_2SO_4 and filtered. All volatiles were evaporated *in vacuo* and the product was obtained after flash chromatography (Hexane : EtOAc = 20 : 1) as a yellow solid (108 mg, 74%); ^{1}H NMR (400 MHz, Chloroform-*d*) δ 12.67 (s, 1H), 8.63 (d, J = 2.8 Hz, 1H), 8.42 (dd, J = 9.2, 2.8 Hz, 1H), 7.76 – 7.69 (m, 3H), 7.61 (t, J = 7.6 Hz, 2H), 7.21 (d, J = 9.3 Hz, 1H); ^{13}C NMR (100 MHz, Chloroform-*d*) δ 200.5, 168.0, 139.5, 136.4, 133.2, 130.9, 129.6, 129.3, 128.9, 119.6, 118.0; HRMS (ESI) calcd for $C_{13}H_8NO_4$ (M - H^+) 242.0459, found 242.0454; Melting point: 121–122 °C.

4.3. Determination of minimum inhibitory concentration (MIC)

The antimicrobial activity of the compounds was determined by broth microdilution according to the CLSI guidelines [21]. The following bacterial strains were used in this study for the microdilution assay: *Enterococcus faecalis* ATCC 29212, *Streptococcus pneumoniae* ATCC 49619, *Klebsiella pneumoniae* ATCC 700603, *Acinetobacter baumannii* ATCC 19606, *Pseudomonas aeruginosa* PA01, *Enterobacter cloacae* ATCC 13047, *Escherichia coli* ATCC 25922. The test medium was brain heart infusion (BHI) for *S. pneumoniae* and Mueller-Hinton broth (MH) for the rest of the organisms. Serial two-fold dilutions were performed for the tested chemicals starting from 256 µg/mL to 0.5 µg/mL, and the bacterial cell inoculum was adjusted to approximately 1.5×10^6 CFU per mL. Results were taken after 16–20 hrs of incubation at 37 °C. The MIC was defined as the lowest concentration of antibiotic with no visible growth. Experiments were performed in duplicates.

4.4. Binding inhibition assay

Previously established protocols were used for inhibitor testing [22]. 40 mL *N*-LgBiT-NusB (2.5 mM in PBS) was added to 96-well plates and then mixed with 20 mL compound. The mixture was incubated for 10 min at 37 °C. 40 mL C-SmBiT-NusE (2.5 mM in PBS) was then added to each well, followed by incubation for 10 min at 37 °C. The final

concentration of the compounds was at 125 mM. After the final incubation step, an equal volume of Promega Nano-Glo® Luciferase Assay Substrate was added to the reaction mixture. Luminescence emitted was measured using a Victor X3 Multilabel plate reader. The experiment was performed in triplicate with technical repeats.

4.5. Time kill kinetics

The time kill kinetics assay was performed using the CLSI guidelines [21]. *S. aureus* cells were suspended to ~ 1.5×10^6 CFU/mL at log phase in MH medium with compounds at various concentrations. As an untreated control, bacteria were incubated in MH medium without compounds. The cultures were grown at 37 °C with shaking at 200 rpm, and 10 μL sample was taken at defined time points (0, 2, 4 and 6 h) for each treatment group, followed by 10-fold serial dilutions. 5 μL sample was taken from each dilution and spotted on a blood agar plate. After incubation at 37 °C overnight, the number of viable bacteria in each sample was counted and expressed as CFU/mL. The experiment was performed in triplicate. Technical repeats were taken to ensure consistent results were obtained.

4.6. Assessment of ATP production

S. aureus cells were suspended to ~1.5×10^6 CFU/mL at log phase in MH medium with compounds at various concentrations. As an untreated control, bacteria were incubated in MH medium without compounds. The cultures were grown at 37 °C with shaking at 200 rpm, and 10 μL sample was taken at defined time points (0, 2, 4 and 6 h) for each treatment group. The ATP production was measured using the BacTiter-Glo™ Microbial Cell Viability Assay Kit (Promega™) according to the manufacturer's instructions. The experiment was performed in triplicate. Technical repeats were taken to ensure consistent results were obtained.

4.7. Confocal microscopy and macromolecular quantitation

B. subtilis strain BS61 (NusB-GFP) [30] was grown on LB agar plate containing 5 mg/mL chloramphenicol. A single colony was incubated in LB medium supplemented with 5 mg/mL chloramphenicol at 37 °C until OD600 ~ 0.6. Compound at 1/8, ¼, ½, 1 × MIC was then added to the culture and allowed to incubate for further 15 min. 2.5 μL of cell culture was placed onto 1.2% freshly made agarose plate and covered with a coverslip prior to imaging. Leica TCS SPE confocal microscope equipped with 63 × /1.3 oil objective and mercury metal halide bulb was used to capture the fluorescence images. The fluorescence images were processed with LAS X software. For macromolecular quantitation, *B. subtilis* stain 168 were grown on LB agar plate overnight and a single colony was inoculated into LB medium. Compound **23** at 1/8 and ¼ MIC were added to the culture at early log-phase (OD 0.2), and cells were harvested at mid-log phase (OD 0.5) by centrifugation. Cell lysis and macromolecular quantitation were performed as described previously [18].

4.8. In vitro cytotoxicity

Human cell lines A549 lung carcinoma and HaCaT immortalized keratinocytes were used in this study. The cells were seeded at 2.5×10^5 per well. After 24 hr incubation, the tested compounds were added in a 2-fold serial dilution ranging from 1.562 mg/mL to 50 mg/mL. The plates were incubated at 37 °C. At 48 hr and 72 hr after adding the compound, the MTT assay was performed as described previously [18]. 5-fluorouracil was used as a positive control and DMSO as a negative control.

4.9. Hemolysis assay

To separate erythrocytes from human whole blood, 35 mL of human whole blood was centrifuged at 500 × g, 4 °C for 5 mins. After centrifugation, the upper layers of plasma and buffy coat were aspirated by micropipette. 150 mM NaCl solution was added to the packed erythrocytes and filled up to the original volume mark, and the solution was gently shaken to re-suspend the erythrocytes. The centrifugation process was repeated with the same condition and after centrifugation, the upper layers were aspirated and discarded, followed by the re-suspension of erythrocytes using PBS (pH 7.4). A 40 × -diluted erythrocyte suspension was prepared by adding 1 mL of the final suspension into 39 mL of PBS (pH 7.4). Compounds with a final concentration of 0.1, 1 and 10 μg/mL were incubated at 37 °C with 2% blood solution in PBS (pH 7.4) for 45 min. 1600 μL of the 40 × -diluted erythrocyte suspension was added to 400 μL of the compound solution in PBS (with 0.5% DMSO). The mixture was vortexed gently for 10 s and inverted several times to ensure a thorough mixing. The prepared mixture was transferred to 96-well microplates for incubation (200 μL per well, n = 6). Positive control was Triton X-100, a known hemolytic agent, with a final concentration of 1% v/v in PBS. Negative control is the vehicle which is PBS (pH 7.4). After incubation, the reactions were terminated by centrifuging the samples 10 min at 500 × g, 4 °C, to pellet the remaining erythrocytes and erythrocyte ghosts. Then, 100 μL of the supernatant from each well was transferred to a new 96-well plate, and the absorbance of the supernatant was measured at 540 nm, which is the hemoglobin absorbance peak, with CLARIOstar microplate reader (BMG Labtech, Offenburg, Germany). % of lysis was calculated with the following equation:

$$\%\ of\ lysis = \frac{A_{sample} - A_{-ve\ control}}{A_{+ve\ control} - A_{-ve\ control}}$$

A_{sample}: absorbance of the tested compound solution; $A_{-ve\ control}$: absorbance of the vehicle solution; $A_{+ve\ control}$: absorbance of the Triton X-100 solution.

4.10. Caco-2 permeability study

Caco-2 cells were cultured at 37 °C in Dulbecco's Modified Eagle Medium with 10% fetal bovine serum, 1% nonessential amino acids, and 100 U/mL penicillin, and 100 μg/mL streptomycin in an atmosphere of 5% CO_2 and 90% relative humidity. The cells were passaged after 90% confluence using trypsin-EDTA and plated at a 1:5 ratio in 75-cm^2 flasks. The cells (passage number: 45) were seeded at a density of 60,000 cells/cm^2 on polycarbonate membranes of Transwells (12 mm inner diameter, 0.4 μm pore size, 1 cm^2; Corning, NY, USA). Medium was changed the day after seeding and every second day thereafter (AP volume 0.5 mL and BL volume 1.5 mL). The Caco-2 cell monolayers were used 21 to 28 days after seeding. Transepithelial electrical resistance (TEER) was measured to ensure monolayer integrity. Cell monolayers with TEER values less than 165 Ω cm^2 were discarded in transport experiments. Transport studies involved only apical (AP) to basolateral (BL) direction. Cell monolayers were preincubated with transport buffer solution (PBS +) for 20 min at 37 °C. To study absorptive transport, the donor (AP) compartment buffer was replaced with 0.5 mL of transport buffer containing 10 μg/mL of compounds. The pH in both AP and BL compartments was maintained at 7.4 for all transport studies. Concentration of MC4 compounds in the receiver (BL) compartment was monitored as a function of time in the linear region of transport and under sink condition (which is the receiver concentration is < 10% of the donor concentration). At each sampling time point, 100 μL of sample was drawn from the receiver compartment, and a same volume of blank buffer was added into receiver compartment. Concentration of compounds in sample solution was determined using LC-MS/MS.

Notes

The authors declare no competing financial interest.

Acknowledgement

The research was supported by the Shenzhen Science, Technology and Innovation Commission (SZSTI) grant JCYJ20170303155923684, China (C.M.), Hong Kong RGC Early Career Scheme grant No. 25100017, Hong Kong (C.M.), State Key Laboratory of Chemical Biology and Drug Discovery, and internal grant G-YBYY, Hong Kong Polytechnic University, Hong Kong (C.M.), Hong Kong RGC General Research Fund GRF No. 14165917, Hong Kong (X.Y.), Hong Kong Food and Health Bureau HMRF Grant No. 17160152, Hong Kong (X.Y.) and Chinese University of Hong Kong, Faculty of Medicine Faculty Innovation Award FIA2018/A/03, Hong Kong (X.Y.).

Appendix A. Supplementary material

Supplementary data to this article can be found online at https://doi.org/10.1016/j.bioorg.2019.103203.

References

[1] M.Z. David, MRSA community pneumonia: a global perspective on resistance, Lancet Infect. Dis. 16 (2016) 1309–1310.
[2] H. Grundmann, M. Aires de Sousa, J. Boyce, E. Tiemersma, Emergence and resurgence of methicillin-resistant *Staphylococcus aureus* as a public-health threat, Lancet 368 (2006) 874–885.
[3] C. Ma, X. Yang, P.J. Lewis, Bacterial transcription as a target for antibacterial drug development, Microbiol. Mol. Biol. Rev. 80 (2016) 139–160.
[4] S.A. Darst, Bacterial RNA polymerase, Curr. Opin. Struct. Biol. 11 (2001) 155–162.
[5] A.N. Keller, X. Yang, J. Wiedermannová, O. Delumeau, L. Krásný, P.J. Lewis, *ε*, a new subunit of RNA polymerase found in gram-positive bacteria, J. Bacteriol. 196 (2014) 3622–3632.
[6] I. Artsimovitch, S.H. Knauer, Ancient transcription factors in the news, MBio 10 (2019) e01547–e1618.
[7] G.A. Belogurov, I. Artsimovitch, Regulation of transcript elongation, Ann. Rev. Microbiol. 69 (2015) 49–69.
[8] A. Das, K. Wolska, Transcription antitermination in vitro by lambda N gene product: requirement for a phage nut site and the products of host nusA, nusB, and nusE genes, Cell 38 (1984) 165–173.
[9] S.W. Mason, J. Li, J. Greenblatt, Host factor requirements for processive antitermination of transcription and suppression of pausing by the N protein of bacteriophage lambda, J. Biol. Chem. 267 (1992) 19418–19426.
[10] N. Said, F. Krupp, E. Anedchenko, K.F. Santos, O. Dybkov, Y.H. Huang, C.T. Lee, B. Loll, E. Behrmann, J. Bürger, T. Mielke, J. Loerke, H. Urlaub, C.M.T. Spahn, G. Weber, M.C. Wahl, Structural basis for λN-dependent processive transcription antitermination, Nat. Microbiol. 2 (2017) 17062.
[11] F. Krupp, N. Said, Y.H. Huang, B. Loll, J. Bürger, T. Mielke, C.M.T. Spahn, M.C. Wahl, Structural basis for the action of an all-purpose transcription anti-termination factor, Mol. Cell. 74 (2019) 143–157.
[12] E. Nudler, M.E. Gottesman, Transcription termination and anti-termination in *E. coli*, Genes Cells. 7 (2002) 755–768.
[13] M. Torres, J.M. Balada, M. Zellars, C. Squires, C.L. Squires, *In vivo* effect of NusB and NusG on rRNA transcription antitermination, J. Bacteriol. 186 (2004) 1304–1310.
[14] K.B. Arnvig, S. Zeng, S. Quan, A. Papageorge, N. Zhang, A.C. Villapakkam, C.L. Squires, Evolutionary comparison of ribosomal operon antitermination function, J. Bacteriol. 190 (2008) 7251–7257.
[15] B.M. Burmann, K. Schweimer, X. Luo, M.C. Wahl, B.L. Stitt, M.E. Gottesman, P. Rösch, A NusE:NusG complex links transcription and translation, Science 328 (2010) 501–504.
[16] N. Singh, M. Bubunenko, C. Smith, D.M. Abbott, A.M. Stringer, R. Shi, D.L. Court, J.T. Wade, SuhB associates with Nus factors to facilitate 30S ribosome biogenesis in *Escherichia coli*, mBio. 7 (2016) e00114–e116.
[17] S.J. Greive, A.F. Lins, P.H. von Hippel, Assembly of an RNA-protein complex. Binding of NusB and NusE (S10) proteins to boxA RNA nucleates the formation of the antitermination complex involved in controlling rRNA transcription in *Escherichia coli*, J. Biol. Chem. 280 (2005) 36397–36408.
[18] X. Yang, M.J. Luo, A.C.M. Yeung, P.J. Lewis, P.K.S. Chan, M. Ip, C. Ma, First-in-class inhibitor of ribosomal RNA synthesis with antimicrobial activity against *Staphylococcus aureus*, Biochemistry 56 (2017) 5049–5052.
[19] X. Luo, H.H. Hsiao, M. Bubunenko, G. Weber, D.L. Court, M.E. Gottesman, H. Urlaub, M.C. Wahl, Structural and functional analysis of the *E. coli* NusB-S10 transcription antitermination complex, Mol. Cell. 32 (2008) 791–802.
[20] Y. Qiu, S.T. Chan, L. Lin, T.L. Shek, T.F. Tsang, N. Barua, Y. Zhang, M. Ip, P.K. Chan, N. Blanchard, G. Hanquet, Z. Zuo, X. Yang, C. Ma, Design, synthesis and biological evaluation of antimicrobial diarylimine and -amine compounds targeting the interaction between the bacterial NusB and NusE proteins, Eur. J. Med. Chem. 178 (2019) 214–231.
[21] CLSI, Clinical and Laboratory Standards Institute, Performance Standards for Antimicrobial Susceptibility Testing, Twenty-Fifth Informational Supplement (M100S25), Clinical and Laboratory Standards Institute, Wayne, PA, 2015.
[22] T.F. Tsang, Y. Qiu, L. Lin, J. Ye, C. Ma, X. Yang, Simple method for studying *in vitro* protein-protein interactions based on protein complementation and its application in drug screening targeting bacterial transcription, ACS Infect. Dis. 5 (2019) 521–527.
[23] G. Pappas, E. Liberopoulos, E. Tsianos, M. Elisaf, *Enterococcus casseliflavus* bacteremia. Case report and literature review, J. Infect. 48 (2004) 206–208.
[24] W.F. Oliveira, P.M.S. Silva, R.C.S. Silva, G.M.M. Silva, G. Machado, L.C.B.B. Coelho, M.T.S. Correia, *Staphylococcus aureus* and *Staphylococcus epidermidis* infections on implants, J. Hosp. Infect. 98 (2018) 111–117.
[25] J. Hur, A. Lee, J. Hong, W.Y. Jo, O.H. Cho, S. Kim, I.G. Bae, *Staphylococcus saprophyticus* bacteremia originating from urinary tract infections: a case report and literature review, Infect. Chemother. 48 (2016) 136–139.
[26] M. Kilian, K. Poulsen, T. Blomqvist, L.S. Håvarstein, M. Bek-Thomsen, H. Tettelin, U.B. Sørensen, Evolution of *Streptococcus pneumoniae* and its close commensal relatives, PLoS ONE 3 (2008) e2683.
[27] S. Watanabe, N. Takemoto, K. Ogura, T. Miyoshi-Akiyama, Severe invasive streptococcal infection by *Streptococcus pyogenes* and *Streptococcus dysgalactiae* subsp. *equisimilis*, Microbiol. Immunol. 60 (2016) 1–9.
[28] V.N. Raabe, A.L. Shane, Group B streptococcus (*Streptococcus agalactiae*), Microbiol. Spectr. 7 (2019), https://doi.org/10.1128/microbiolspec.GPP3-0007-2018.
[29] M.A. Lobritz, P. Belenky, C.B. Porter, A. Gutierrez, J.H. Yang, E.G. Schwarz, D.J. Dwyer, A.S. Khalil, J.J. Collins, Antibiotic efficacy is linked to bacterial cellular respiration, Proc. Natl. Acad. Sci. USA 112 (2015) 8173–8180.
[30] G.P. Doherty, D.H. Meredith, P.J. Lewis, Subcellular partitioning of transcription factors in *Bacillus subtilis*, J. Bacteriol. 188 (2006) 4101–4110.
[31] C. Li, L. Zhang, L. Zhou, S.K. Wo, G. Lin, Z. Zuo, Comparison of intestinal absorption and disposition of structurally similar bioactive flavones in *radix scutellariae*, AAPS J. 14 (2012) 23–34.
[32] http://biosig.unimelb.edu.au/pkcsm/prediction, accessed on July 7, 2019.